Quantifying Nuclear Deformation and Masses

By

Taghreed Muslih AL Qurashi

Abstract

The scope of this dissertation is to unfold a distinct and detailed analysis regarding the quantification of nuclear deformation over a broad spectrum of nuclear mass numbers, A. Several basic current nuclear models are introduced and explained that provide an insight on nuclear structures. This is followed by an investigation of the nuclear 2^+ and 4^+ excited state transition energies of even-even nuclei. By using the information yielded from the E (2^+), E (4^+) excitation energies and their respective R (4/2) ratio, the respective values of the moments of inertia were shown to be a result of the nuclear deformation. The extracted deformations were investigated using the respective moments of inertia and also the nuclear product valence correlation ($N_p.N_n$) scheme. Moreover, the data were manipulated in such a way that the existence of magic (and doubly magic) numbers were clearly evident at N,Z=2, 8, 20, 28, 50, 82 and 126, corresponding to nuclear shell closures. Finally, it is shown that the ratio of the E (4^+) energy to the E (2^+) energy has a value of 3.33 for a perfect rotor and a value of closer to 2.0 for an idealised vibrational nucleus, and a value of < 2.0 for a near closed shell/near magical nucleus. The results demonstrate the importance of valence nucleons which are the main contributors to the evolution of nuclear deformation.

Acknowledgments:

First of all, my thanks should go to Allah who creates us from nothing. I would like to express my utmost thanks and appreciation to my supervisor, Prof. P.H Regan for his invaluable, unlimited help, support, advice and guidance during the term of my dissertation. His constant enthusiasm, help, encouragement, dedicated corrections during the time of writing up, and his patience are much appreciateds, of course without his all support this thesis would have never completed. I would like also to give my greatest gratitude and thanks to Dr.Stevenson PD for his continuous support, help and guidance, as without his advice and his keenness in giving all valuable knowledge, expertise my Msc would not be completed. My special gratitude extended to Mrs Jane Clarke and all staff and colleagues at the Faculty of Engineering and Physical Sciences for their invaluable advice and help in Reality they made me feel home as their friendly attitude, kind living and communicating. Also my great thanks extended to my Parents my mother Samiah and my father Muslih for their being there all the time for me. Last, but certainly not least, I would like to express my huge thanks to my Love husband and his kind family for their support and help , and my daughters Taleen and Sireen for their patience. Also, I would like to give my thanks to my best friend Abeer for her kind help and support during the hard time.

1. *Introduction*

The search for the elements that constitute the fundamental nature of matter has its origins back to the ancient Greeks. In fact, it was a Greek philosopher, Democritus that first introduced and subsequently developed the idea that all living matter is in fact composed by tiny bits which he consequently called 'atoms' (Walker J., 2004, Campbell MK. and Goldstein N., 2012). *Despite the fact that this novel idea of atoms was highly revolutionary and innovative, it was soon abandoned because it was plainly thought of as being an unrealistic figment of Democritus' imagination. Therefore, it was not before the beginning of the 19th century and Dalton's successful experiments that this idea was revisited and, consequently started becoming prevalent and widely accepted. Dalton had now clear evidence that distinctly proved and demonstrated that matter indeed seemed to consist of fine and elementary particles (Demtrųder* W., 2010, Olmsted J. and Williams GM., 1997). *However, it was the discovery of radioactivity by Becquerel in 1896 that essentially triggered the development of the novel, yet fascinating field of nuclear physics, a field that revolved around nuclear characteristics and interactions. Furthermore, the subsequent discovery of electron by JJ Thompson in 1897 and the interpretation of the famous scattering experiments performed by Geiger and Marsden by Rutherford in 1911 additionally propelled the basic interpretation of the atomic structure. All positive charge and almost all of the atomic mass are concentrated in the central (nucleus), whereas, on the other hand, the negatively charged electrons were surrounding that centre on distinct orbits (de Gruyter* W., 1997, Niaz M., 2009). *Nevertheless, the study of radioactivity was relatively low profile until the 1930s and it was primarily limited to medical research e.g. radiation therapies for cancers (Reed BC., 2013). Hence, it was the discovery of neutron in 1932 and the subsequent Fermi's neutron bombardments experiments that rendered nuclear physics as a high-profile domain of research (Mason TE. et al, 2013). In fact, Chadwick's discovery allowed for the correct identification of the constituents of nucleus: positively charged protons and electrically neutral neutrons. The nucleus is thus determined by its charge number Z (defined by the number of protons) and its mass number A (which is, in turn, defined as the total number of neutrons plus protons). Elements that have the same atomic number of Z but different neutron number N are known as isotopes, whereas on the other hand, elements that have the same N but different Z are known as isotones (Martin B., 2011, Kakani SL., 2006).*

1.1. Scope of this dissertation

In this dissertation the nuclear structure is explicitly described through the investigation of some of the properties of nuclei including the energy of the excited states and the rotation and vibrational states of the respective deformed nuclei. The primary focus will revolve around the so - called Yrast[i] states with angular momentum and parity quantum numbers 2^+ and 4^+. These correspond to the nuclear excited state energies of even □ even nuclei (i.e., nuclei with even number of protons and even number of neutrons). It should be noted that the rotational characteristics of nuclides have been long exhibited by Bohr. In fact, Bohr stated that measurements of rotational nuclei are possible due to their deformation which, in turn allow for a change in the position or point of reference (Hellem J., 2008, Blaum K. et al, 2013). Nevertheless, some of the basic current models will be discussed and unfolded that describe the nucleus and the respective nuclear structure. For instance, the shell model defines that the motion of each and every nucleon is directly influenced by the average force (attractive) of the other nucleons (Krane KS., 1998). Hence, the respective orbits are by default forming shells. As a result of this model magic numbers are predicted that represent shells which are 'filled'. On the other hand, the collective model accounts for valence nucleons that have been shown to collectively cause deformation as compared to the normal spherical shape
(Khagram P., 2007). The decays from the $I^{□}=2^+$ and 4^+ excited states in
$R = 2.0$ for an idealised vibrational nucleus; and it should be $R < 2.0$ for near closed shell / near magic nuclei. These deformations were analysed using the respective moments of inertia and also the nucleon product valance correlation scheme (the N_pN_n scheme).

Nuclear Structure and Decay Theory and Models

2.1.Nucleus and the Nuclear Chart

Each element consists of different isotopes; atoms whose nuclei have the same Z but different N values (Lilley J., 2002, Durrant A., 2000). Advancements in

the field of accelerator technology have allowed nuclear scientists to extend their research on new isotopes that are far from their respective stable isobars. One of the most essential goals of nuclear physics is the production and identification of new elements that will, in turn, redefine the existing periodic table (Bowler MG., 1973). Therefore, it comes as no surprise that this in depth study of the new nuclides has led to a massive expansion and acquisition of the available nuclear data. In fact and according to the National Nuclear Data Centre (NNDC), the total number of nuclides for which data is currently available exceeds the 3000 (nndc.bnl.gov, 2015). However, out of the approximately 7000 nuclides that are thought to possibly exist there are only 286 proton □neutron combinations that are able to produce effectively stable nuclei (physicsworld.com, 2011). For instance, tin (Z = 50) has 10 stable isotopes, whereas technetium (Z = 43), promethium (Z = 61) and polonium (Z = 84) have none. Nevertheless, a nuclear chart essentially depicts all these nuclei which are, in turn, plotted with respect to their Z and N values (Winn W., 2010). Figure 1 shows such a nuclear chart in which the black area indicates stable nuclei (i.e. those that lie along the line of stability in the Segrй chart), and the yellow area indicates the area of all known nuclei.

Furthermore, an area defined as 'Terra incognita' illustrates the 'zone' where the existence of nuclei has been assumed. Despite the fact that this area is not yet experimentally supported it is of utmost importance for comprehending the production of heavy nuclei.

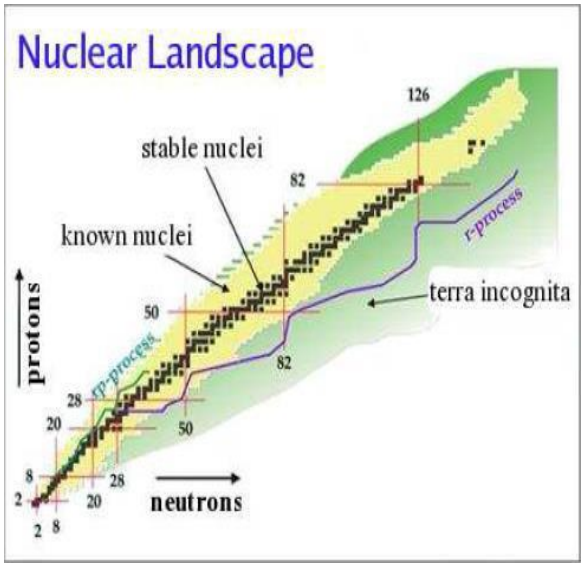

Figure 1. The nuclear landscape. Black dots represent the area of stability, yellow area denotes the area of known yet unstable nuclei, and green represents the regions where the existence of nuclei is practically assumed. Image taken from (Behrens T., 2009)

2.2.Nuclear Stability

However, a very essential aspect of figure 1 deals with the stability of nuclei and their respective ratio of protons vs neutrons. At lower masses (light nuclei) nuclear stability is found where the ratio of neutrons vs protons is 1:1. On the other hand, isotopes with a greater neutron number than the stable ones are bound to become unstable by means of β^- decay, whereas isotopes with a greater proton number will become unstable by β^+ decay or electron capture (Walther J., 2009, Jevremovic T., 2009). However, and as the proton number is increased, the stable isotopes tend to have an increasing ratio of neutrons vs protons in their nucleus. In fact, heavier nuclei are most stable with $N > Z$. . Figure 2 demonstrates the values for N and Z for 266 stable nuclides.

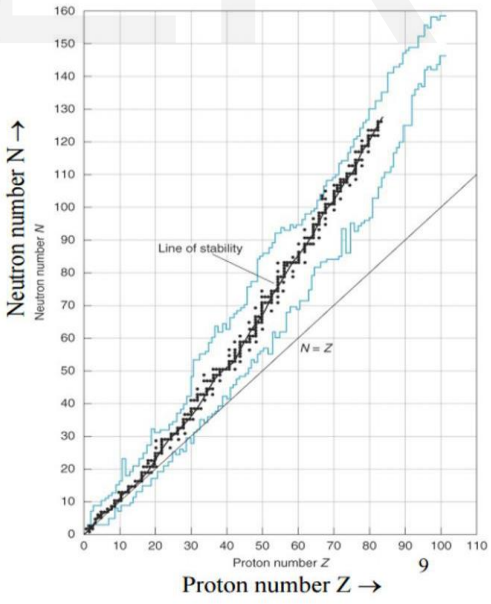

Figure 2. Values for Protons and Neutrons regarding the 266 primoridial, stable nuclides. Graph taken from (web.utk.edu, 2013).

In order to explain this we first need to take into consideration the binding forces (energy required to

'break' into its constituent parts) within the nucleus. The nucleus is essentially held together by the application of a short range force, namely the strong force. In fact, the short range of this force is understood due to the fact that it is operating at distances between 1 fm and 2 fm, where fm = 10^{-15} m as shown in figure 3 (Van Oers WTH., 1992). At such distances the strong force highly overcomes the repulsive Coulomb potential (that is applied between the positively charged protons) and is responsible for holding the nucleons together with a very small (and necessary) separation. In fact, 'the spin - isospin independent attraction of about 50 – 100 MeV in this region plays an essential role to nuclear binding' (Hatsuda T., 2011, pp. 1). In other words, the strong force is charge asymmetric and does not distinguish between the spin states (parallel or anti - parallel) of the respective nucleons. Nevertheless, the nature of this short range force implies that each nucleon needs to move in an almost spherical potential which effectively comes as a result of the average interaction between the given nucleon and its surrounding ones.

Several nuclear models have been proposed and which attempt to adequately explain nuclear stability and the binding energy of the nucleus as it is shown in the next section.

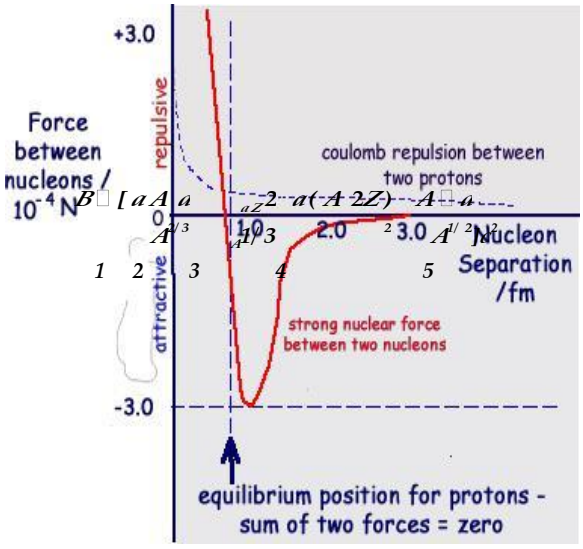

Figure 3. Strong force is repulsive at distances below 0.5 fm and then attractive at greater distances Image taken by (cyberphysics.co.uk, 2015).

2.3. Nuclear Models

All theoretical nuclear models eventually face two principal limitations (Rowe D. and Wood J., 2010). The first limitation deals with the fact that there is currently no exact and precise mathematical expression that describes nuclear forces, as opposed to atomic ones. On the other hand, the second limitation emphasises on the fact that there is no mathematical solution to the many-body problem. However, and despite of these limitations, there have been several nuclear models that have been introduced and that can accurately describe nuclear and atomic properties. The most important of these models are the Liquid Drop model, the Shell model, and the Collective model.

2.3.1. The Liquid Drop Model and the Semi - empirical Mass Formula

The Liquid Drop model is a simple model describing the binding energy of a nucleus. This model was introduced as an accurate nuclear model due to the fact that a liquid drop has constant density which is independent of the number of molecules (Brown GE. et al, 2010). Until the 1930s, and following the experimental measurements of a substantial number of atomic masses, density and nuclear binding energy were found to be approximately the same for all stable nuclei (Patel SB., 2006). In principle, the energy that is required in order to remove molecules from a liquid is defined as the heat of vaporisation which is, in turn, directly proportional to the number (mass) of molecules within the liquid (much like the binding energy is proportional to the mass of nucleons). Hence, and in proportion to this analogy, the Liquid Drop model was introduced to explain nuclear binding energy and in which the nucleons are considered to be distributed in a fairly uniform manner (Yarwood J., 1973). As a result of this theory, Weizsacker developed his semi - empirical mass formula (SEMF) in 1935 (eq. 1) which, in turn, describes the mass of the nucleus, and, thus its binding energy, in relation to A and Z.

$$B = [a_A A - a_S A^{2/3} - a_C \frac{Z^2}{A^{1/3}} - a_{sym}\frac{(A-2Z)^2}{A} + \delta(A,Z)] \quad Eq.\ 1$$

According to the SEMF the short range force is valid (or effective) to particles only when it comes to their direct neighbours. Therefore, the binding energy

within the nucleus solely depends on the numbers of nucleons that reside inside it (Jelley N.A., 2007).

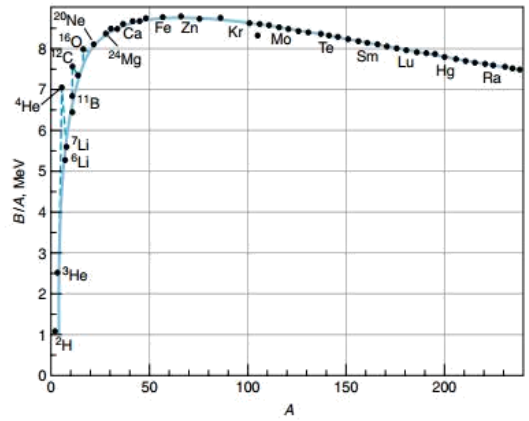

Figure 4. The binding energy per nucleon as a function of the atomic mass number A. The solid curve illustrates the Weizsacker SEMF. Image taken from (ifm.liu.se, 2015)

The first term of equation 1 states that the number of interactions is proportional to A, and it, hence defines that the binding energy is practically constant. The second term is a minor correction to the first one and it primarily accounts for the fact that nucleons that exist on the surface of the nucleus will eventually have a smaller number of neighbours (and, thus a smaller total binding energy). It should be noted that this term comes in total accordance to the surface tension of liquid drop analogy (ifm.liu.se, 2015). Therefore, the nuclear equivalent of the surface tension should be

where $\square_2$ is the respective coefficient (constant) in the Weizsacker formula presented earlier. On the other hand the third term accounts for the positive electrostatic energy of a charged drop (due to Coulomb repulsion which, therefore resists the nuclear trend towards a spherical shape), whereas the fourth one is simply quantum - mechanical based term that was added in

order to account for the fact that in cases where the number of protons is not equal to the number of neutrons the energy if the nucleus is found to increase. Hence, the binding energy will, in turn decrease as a result of the exclusion principle. Finally, the last term incorporates an empirical account for the pairing tendency of the respective nucleons. It should be noticed that the success of this model was due to the fact that it accurately defined the respective limits of stability as a result of particle emission or fission (Hellem J., 2008). Nevertheless, and throughout the last decades, this model has undergone several changes such as the description of the collective excitations as a result of rotations and vibrations. However, the failure of this model in terms of insufficiently explaining the microscopic effects observed in the nucleus propelled the introduction of additional nuclear models such as the *Shell model* and the *Collective model* (Moody K.J. et al, 2005).

2.3.2. The Shell Model

As opposed to the previously mentioned *Liquid Drop model*, the *Shell model* defines that the motion of each and every nucleon comes as a result of the average attractive force of all the other nucleons (and not simply as a result of the neighbouring ones) (Brown G.E. et al, 2010). This is exactly why the respective orbits form what is called '*shells*' (Krane K.S., 1998). It should be mentioned that the evidence of this model stemmed from the same limitations stated in the *Liquid Drop model*: the failure of the *Liquid Drop model* to explain the microscopic effects witnessed in the nucleus. This limitation is, therefore providing clear evidence of the quantum shell structure of the nucleus According to the Pauli principle each nucleon possesses its own distinct set of quantum numbers that essentially define it

$$\square \quad \frac{\square^2}{4\square R^2} \qquad \textit{Eq. 2,}$$
$$A$$

(Abadi Vahid M.M. et al., 2015). Hence, and as more and more nucleons are added in the nucleus, they will need to reside in the lowest possible energy level. Additional evidence that propelled the widespread use of this nuclear model was the extra binding energy that was observed in cases where either the proton or the neutron numbers was equal to 28, 50, 82, and

Moreover, and as it will be shown in the results section of this dissertation, this model is also supported by the prerequisite amount of energy

needed to excite nuclei that contained the so-called magic number of protons or neutrons. These magic numbers (2, 8, 20, 28, 50, 82, 126...) denote the specific number of nucleons that are needed for a full shell (all possible sets of quantum numbers have been occupied) (Rodriguez-Guzman et al., 2015). It should be mentioned that nuclei which have magic numbers for both their neutrons and protons are called doubly magic (Hinke CB. et al, 2012, Rydin R., 2011). As shown in figure 5 there is a considerable amount of spin-orbit interactions that split the levels by a number that is directly proportional to the orbital quantum number and is responsible for the overlapping levels observed (Neeraj M., 2011). Figure 5 also shows that the most stable atoms are (as expected) the noble gases.

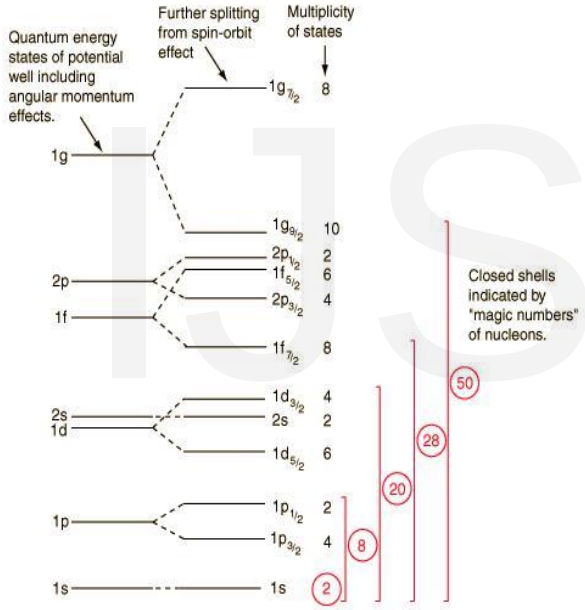

Figure 5. Diagram depicting a comparison between atomic energy levels and the energy levels as defined by the nuclear shell model. Image taken from (hyperphysics.phy-astr.gsu.edu, 2015)

2.3.3. The Collective Model

Collective models were developed in response to the fact that nuclei are not stationary; on the contrary, nuclei show shape and phase evolution (Nakatsukasa T., 2012). The main focus of this dissertation is the quantification of nuclear deformation. Therefore, it goes without saying that changes in the shape of the nucleus involve many nucleons (many nucleons acting together = collectively). The development of the collective behaviour in nuclei comes as a result of correlations among valence nucleons. Therefore, and as opposed to the pure shell model as discussed earlier, collective models (configurations) assume that wave functions are mixed and, thus they are linear combinations of several components (uni-koeln.de, 2015). In other words collective models assume that apart from the individual nucleons that manage to change orbits (and, thus create exited states of the nucleus) there are additional nuclear transitions that involve many other nucleons. Nevertheless, there is a plethora of well - established examples of collective excitations that provoke either oscillation or/ and rotation (Bohr A. and Mottelson B., 1955).

- *Collective Excitations*

First of all, it should be noticed that collective excitations have a predominant effect in medium-mass to heavy nuclei that lie in the areas between the magic numbers (Khagram P., 2007). Hence, nuclei that demonstrate collective behaviour patterns are primarily those with a large mass and with a proton or neutron number that is not near to the magic numbers (filled shells) (Stock R., 2006). This is an extremely logical assumption because in these regions the large number of valence nucleons promotes a collective behaviour where each nucleon affects each other (and, thus triggers a collective influence). However, and owing to the effect of valence nucleons, valence correlation schemes such as the N_pN_n scheme are usually used. The N_pN_n scheme provides the means for parameterising nuclear data in a way that highlights the valence p - n interaction (Casten R., 2000). In fact, and by firstly assuming that the p-n interactions are fairly long range in addition to the fact

that they are solely the ones responsible for the onset of collectivity, configuration mixing, and deformation in nuclei, then the total valence p-n strength will scale with the product of N_pN_n; The Np.Nn (or Nn.Np) value is of absolute importance due to the fact that the interactions between protons and neutrons in highly overlapping orbits are widely accepted to be extremely important parameters in terms of nuclear deformation and their respective phase transitions (Casten RF., 1985)

The significance of a N_pN_n scheme is illustrated in figures 6 and 7 where data from A = 130 region are plotted against the E_{2+} and E_{4+} / E_{2+}. A comparison between plotting N and N_pN_n highlights the simplicity and utility of this scheme.

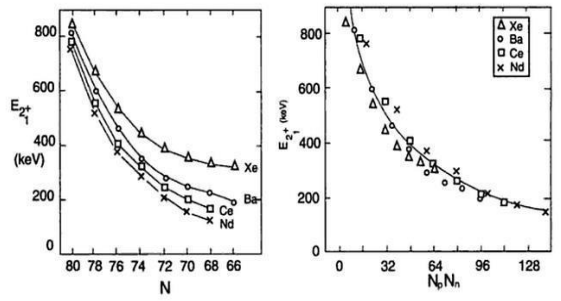

Figure 6. Normal (left) and N_pN_n (right) plots of $E(2^+)$ for the A = 130 region. Image taken from (Casten R., 2000).

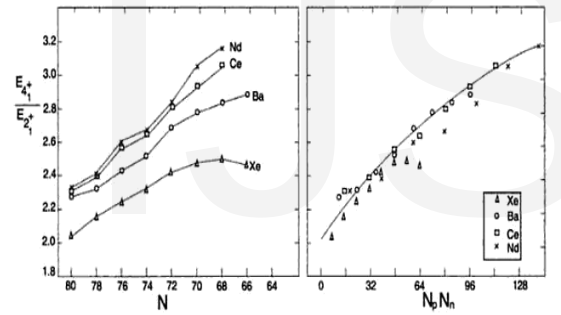

Figure 7. Normal (left) and N_pN_n (right) plots of $E(4^+)/E(2^+)$ for the A = 130 region. Image taken from (Casten R., 2000)

A very useful and sensitive method for measuring the internal structure a nucleus is the measurement of the excitation of the nucleus to the very first excited state. Due to the strong pairing force, even □ even nuclei do not tend to exhibit single particle excited levels and, thus exhibit the simplest systematics (Hellem J., 2008). Even-even nuclei exhibit either one or two particle hole excitations or two quasi particle excitations at low excitation energy. Hence, what we expect is that all even-even nuclei will have ground states with a spin/ parity of 0^+ (Krane KS., 1998). On the other hand, the first excited state of even-even nuclei is expected to have spin/ parity value of 2^+; however, and according to the literature, this is not the case for ^{14}O, ^{16}O, ^{14}C, ^{40}Ca, ^{68}Ni, ^{72}Ge, ^{72}Kr, ^{90}Zr, ^{96}Zr, ^{98}Zr, ^{98}Mo, ^{146}Gd, ^{182}Hg, ^{186}Pb, ^{188}Pb, ^{190}Pb, ^{192}Pb, ^{194}Pb and ^{208}Pb (Raman S. et al., 2001). Nevertheless, there are two major types of collective nuclear behaviour that depends on the size of the nucleus. In fact, for A < 150 the various nuclei vibrate about a spherical equilibrium (vibrational), whereas for nuclei with 150 < A < 190 or A > 220 they instead express a rotational behaviour as a result of their non-spherical shape at equilibrium (Regan PH. et al., 2003).

- *Nuclear Vibrations*

The Liquid Drop model can give us a pretty good idea regarding the way with which a nucleus vibrates. However, the energy of a nucleus, as a quantum system, needs to be quantised (van Dommelen L., 2013). In fact, and by taking into consideration the classical

expression for the lowest frequency we get that

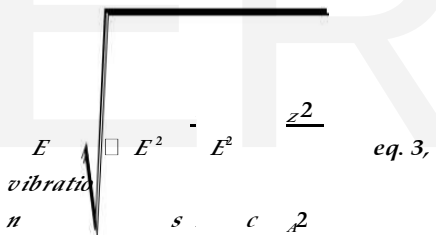

where Es, Ec represent the relative strength of the surface tension and the relative strength of the Coulomb repulsions, respectively for the lowest frequency. The instantaneous shape of the nuclei is non-spherical, as opposed to the spherical average shape. Therefore, the slightest deformation in the shape from the equilibrium is bound to increase the energy of the surface. In fact, and according to Lilley, a small deformation is bound to induce a parabolic energy potential (Lilley J., 2001). Figure 8 illustrates the shape of the barrier as a function of the deformation or fragment separation for several values of atomic mass number A. It is shown that at large separations the shape of the barrier is defined by the Coulomb potential between the charges of the nuclei. A measure of these charge distribution deviations from the spherical shape are defined as the quadrupole moment (Q) of the distribution (cdfe.sinp.msu.ru). On the other hand, and at small deformations (distortions) both terms of eq. 3

compete to each other, where surface tension is trying to pull the nucleus back to its original spherical shape.

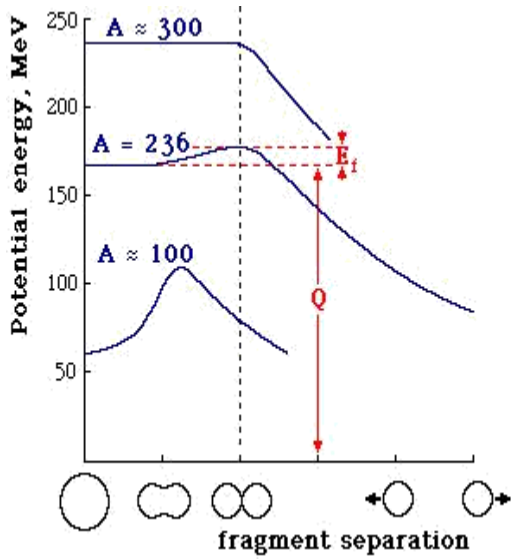

Figure 8. The respective shape of the barrier as a function of the deformation or fragment separation. Image taken from (shef.ac.uk, 2003)

Nevertheless, the instantaneous shape of the nucleus can be described by a radius vector $R(\theta, \varphi)$ as a function of time (t) with θ and φ defining the angular coordinates of a point that resides at the surface

$$R(t) = R_{av}[1 + \beta_2 \cos(\omega t) Y_{\lambda,m}(\theta, \varphi)] \qquad \text{eq. 4,}$$

where β_2 is the deformation parameter, R_{av} is the average radius of the nucleus (which is directly proportional to $A^{1/3}$ (Pearson J., 2008). On the other hand, the term $Y_{\lambda,m}$ introduces angular momentum and figure 9 shows the respective vibrational models for three distinct values of λ (λ= 1, 2, and 3) (Trentalage S. and Koonin E., 1980).

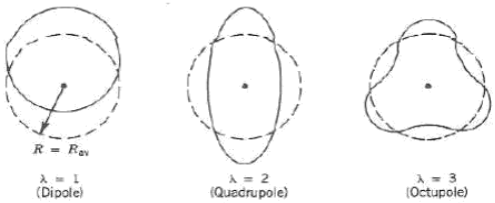

Figure 9. The three lowest vibrational states (modes) of a nucleus. Image taken from (Krane KS., 1998)

For $\lambda = 1$ we have a dipole excitation. In this case the spherical harmonic changes from the center of the mass without the application of external forces. Moreover, what is observed in this state is a highly collective dipole excitation that has a spin / parity of 1^- at excitation energies of 10 - 20 MeV (Lilley J., 2002) On the other hand, and for $\lambda = 2$, we have a quadrupole where all nucleons contribute to the motion of the nucleus. This mode is the lowest vibrational mode and does not call for compression or separation of protons and neutrons. Finally, and for $\lambda = 3$ we have an octupole with an overall negative parity. Such vibrational states are typically observed at energies that are greater than the E2 vibrational states.

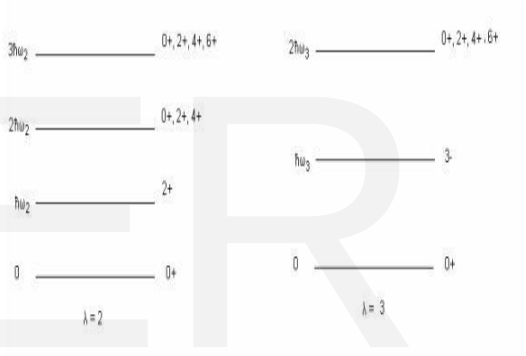

Figure 10. Energy spacing of both quadrapole and octupole phonon excitation of a spheroid

Figure 10 illustrates the energy spacing of both quadrupole and octupole phonon excitation of a spheroid.

- *<u>Nuclear Rotations</u>*

Collective nuclear rotation can be only observed in nuclei that have non-spherical equilibrium shapes. For instance, and according to the principles of quantum mechanics, nuclei that lie close to the magic numbers are practically spherical and, thus rotation is by default forbidden. It was previously stated that nuclei with 150 < A < 190 or A > 220 they express a rotational behaviour as a result of their non-spherical shape at equilibrium (as opposed to nuclei

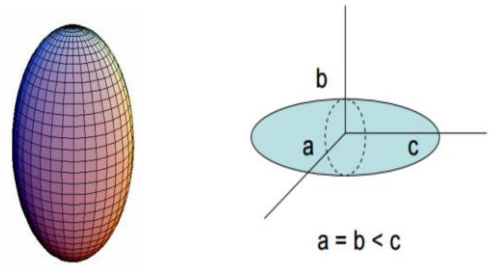

Figure 11. The shape of an axial symmetric prolate ellipsoid that is defined by its semi-major axis. In this case c is greater than the semi-minor axis. Figures taken from (Ovenden C., Khagram P., 2007)

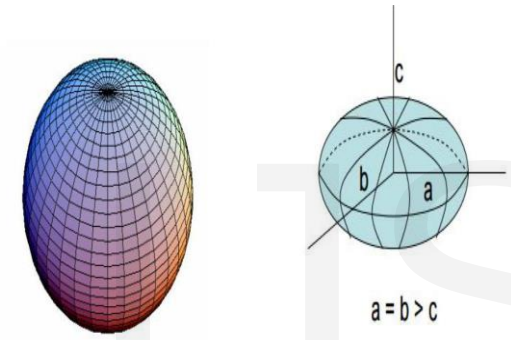

Figure 12. The shape of an oblate ellipsoid that is defined by its semi-major axis. In this case c is smaller than the semi-minor axis. Figures taken from (Ovenden C., Khagram P., 2007)

with A < 150 in which case they vibrate about a spherical equilibrium (vibrational)). These nuclei are, hence called as deformed nuclei and they are ellipsoidal: either prolate or oblate (see figures 11 and 12). However, and in both cases, the nuclei exhibit symmetry about both semi-major and semi-minor axis. Nevertheless, and as previously mentioned, the shape of the deformed nuclei can be described by an ellipsoid as in equation 4, where β is the deformation parameter. The relationship between this parameter and the eccentricity of the respective ellipse is given by equation 5

$$\beta \approx \frac{4}{3}\sqrt{\frac{\pi}{5}}\frac{\Delta R}{R_{average}} \quad \text{eq. 5,}$$

where $R_{average} = R_0 A^{1/3}$ and R describes the difference between the semi major and semi minor axis for the ellipsoid (Alder K. et al, 1956). The parameter β defines the degree to which a nucleus is deformed (its eccentricity). Therefore, when β takes positive values the respective nucleus is deformed like a prolate ellipsoid (figure 11), whereas in cases where β takes negative values the respective nucleus is oblate (figure 12).

- *Moment of Inertia*

The kinetic energy for a rotating object is given by

$$E = \frac{1}{2}\zeta\omega^2 \quad \text{eq.6,}$$

Where ζ is the moment of inertia (rotational mass), and ω is the angular velocity of the object. Taking into consideration that the angular momentum is, in turn equal to ζω then equation 6 becomes

$$E = \frac{I^2}{2\zeta} \quad \text{eq. 7,}$$

Hence, and by simply replacing the value of angular momentum I with the angular momentum quantum number we get that

$$E(I) = [\hbar^2/2\zeta]i(i+1) \quad \text{eq. 8.}$$

Equation 8 shows that the rotational energy of a given nucleus is increasing in proportion to the angular momentum quantum number.

However, this equation is also very important for the purposes of this dissertation because it provides the energies of even - even nuclei (rotating objects) in quantum mechanics. Hence, and when considering the 2^+ energy state (where i = 2) we get that $E(2^+) = 6(\hbar^2/2\zeta)$. Accordingly, and by replacing the appropriate values for i, we can get the values for the other energy states as shown below. It should

be mentioned that the ground state of even □even nuclei has always a value of 0.

$E(0^+) = 0$

$E(2^+) = 6(\hbar^2 / 2\zeta)$

$E(4^+) = 20\,(\hbar^2 / 2\zeta)$

$E(6^+) = 42(\hbar^2 / 2\zeta)$

$E(8^+) = 72(\hbar^2 / 2\zeta)$

Figure 13. Energy for even - even nuclei at the respective ground or excited states

Nevertheless, an important element of figure 13 is the ratio $E(4^+) / E(2^+)$ because on one hand it eliminates the dependence on moment of inertia and on the other hand, sets the upper limit of 3.33 for this ratio. This number is characteristic for nuclides that are known as perfect rotors.

Figure 14 in turn illustrates the ground state rotational band that is formed as a result of these nuclear excited states in the form of energy level diagrams.

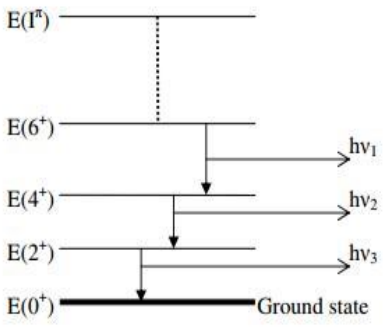

Figure 14. Schematic energy level diagram illustrating the sequence formed by nuclear excited states

The moment of inertia can also be written as a function of the nuclide's mass and radius as in equation 9.

□□□□□□□r^2 9,

where κ represents a proportionality constant and can be used in order to define the respective nuclear deformation. Therefore, and by taking into consideration the dependence between the radius and the atomic mass we get,

□□ □□□□□ r^2 □□ (r □ $1.2\,A^{1/3}$ fm, M □ A)

□□ □□ $A^{5/3}\,u\,fm^2$

where u is the atomic mass unit.

2.4. Nuclear deformation and its determination from the experimental decay lifetimes of the 2^+ Yrast state nuclei

A very accurate and sensitive method of measuring the stability of the various nuclei is to experimentally collect values for the reduced electric quadrupole transition probability B(E2)↑ between the 0^+ ground state and the first 2^+ excited state in even □even nuclides (Raman S. et al., 2001). In fact, and in cases where the nuclei under investigation are deformed, this probability directly depends on the magnitude of the intrinsic quadrapole moment Q_0 (and, thus on deformation) (Hossain i. et al, 2014). In fact, this probability is, in turn, given by the inverse of the lifetime of the given excited state τ (Raman S. et al., 2001, Hellem J., 2008) The accumulation of the B (E2)↑ values can be obtained by means of Coulomb excitation and inelastic electron scattering. These values can also be acquired by means of measuring the lifetimes of the respective excited states, a method which is very suitable in our case due to the fact that we are dealing with high spins (Longo L., 2015). The experimental decay lifetimes of nuclei is an additional, yet equal, indicator of the respective nuclear structures.

According to Raman, the B (E2)↑ values and the τ values are related through equation

11 (Raman S. et al., 2001):

13 5 □(□ 2)□ $_1$

□ (1 □) □ □ $_0$ □□ [_____] eq. 11

40.81×10

$e^2 b^2$

where α is a constant (internal conversion coefficient) that depends on the specific value of E,

E is defined in terms of keV, B(E2) in terms of e^2b^2 ($e = 1.6 \times 10^{-19}$ J, $b = 1 \times 10^{-28}$ m^2) and τ

is the mean lifetime of the state in picosecond. It should be noted that the reduced electric quadrupole transition probability values are fundamental experimental quantities and are independent of the nuclear models. In contrast to the B (E2)↑ values, the deformation parameter β is model dependent. However, and owing to its easy visualization this parameter is of utmost importance to the quantification of nuclear deformations. In fact, and assuming a charge distribution that is uniform up to a distance of R (θ,φ) but takes the value of zero beyond that, the deformation parameter can be related to the B (E2)↑ values by the following equation (Raman S. et al., 2001)

$$\beta = \frac{4\pi}{3ZR^2}\sqrt{\frac{B(E2\uparrow)}{e^2}} \quad (4)$$

where Z represents the atomic charge of the nucleus.

3. Results

3.1. Yrast 2^+ energies of even-even nuclides

It was previously stated that the lowest excited state of most even-even nuclides is a spin/parity 2^+ state. The data of the 2^+ energy state were collected from the literature and they are consequently plotted as a function of the respective proton and neutron numbers as shown in figure 15 (nndc.bnl.gov, 2015). Appendix 1 provides a full list of all values collected for all nuclides regarding their 2^+ and 4^+ energies together with their respective proton, neutron, and mass numbers. Nevertheless, and despite the fact that the respective shape of the graph does not at first indicate any order or useful conclusions regarding the reasons for the appearance of spikes in excitation energy, it can be easily inferred that the sudden increase in

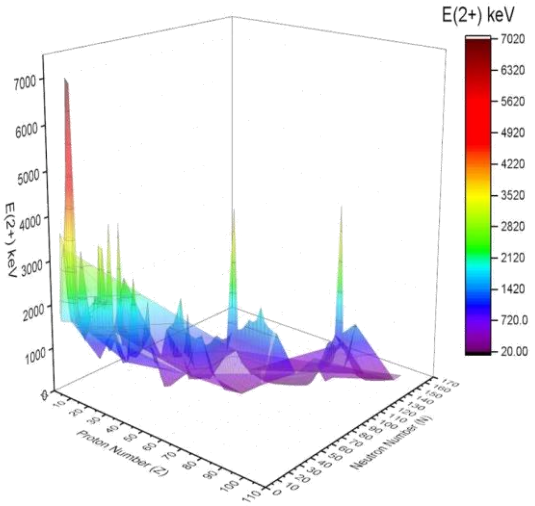

Figure 15. 2+ Yrast 2^+ Excitation Energies for even-even nuclei plotted as a function of N and Z

the excitation energy of certain nuclei can be attributed to the theoretical predictions where a full shell will always translate into a highly stable nuclide (Bryan J., 2013, Magill J. and Galy J., 2005). These spikes are in accordance to the magic numbers are 2, 8, 20, 28, 50, 82, and 126 and, hence correspond to full shells (in total agreement to the nuclear shell model that was discussed earlier). The first couple of spikes that are exhibited to the left of figure 15 belong to ^{16}O (8 protons and 8 neutrons) and the alpha particle ^4He (2 protons and 2 neutrons), $^{12}C_6$ (six protons and six neutrons), $^{14}C_6$ (six protons and 8 neutrons). On the other hand, the two large spikes to the right of the graph correspond to ^{132}Sn and ^{208}Pb nuclides. Hence, it can be easily seen that these nuclides have excitation energies that are either double (tin) or quadruple (lead) compared to those of their respective neighbors. Therefore, and going back to figure 15, the large spikes observed correspond to nuclides that are either magic or doubly magic (isotopes with both proton and neutron numbers matching the magic ones). The high energies of up to 7 MeV correspond to the nuclides $^{12}C_6$, $^{14}C_8$, $^{132}Sn_{82}$, $^{40}Ca_{20}$, $^{14}O_8$, $^{16}O_8$ and $^{208}Pb_{126}$. Moreover, it can be also observed that the heavier the nuclei in our graph the lower the excitation energy becomes and, thus the more unstable they are (areas of high deformation that are especially found in the region between the two pikes to the right of the graph in figure 15). An additional characteristic of figure 15 is the behavior of the ^{32}Mg nucleus. According to the mean field framework, the

^{32}Mg nuclide is theoretically predicted to have a spherical ground state (Rodriguez-Guzman et al., 2015). However, and according to the acquired experimental value of the first excited state B (E2, $0^+ \rightarrow 2^+$) (and as we will see later also due to the ratio R (E_{4+} / E_{2+})) it is suggested that this is not true and that this nuclide demonstrates in fact a deformed ground state. This weakening (or erosion as described in the literature) is characteristic of the N = 20 and N = 28 magic numbers in nuclei that are light and have a rich consistency of neutrons (plain mean field approximations (Ring P. and Schuck P., 1980)). Hence, such challenging shell effects with respect to neutron rich nuclei, are in contradiction with the accumulated experience regarding stable nuclear systems (Michimasa S. et al, 2014).

In fact, and according to a paper published from Nakada and Sugiura in 2014, 'although deformation degrees of freedom are not explicitly taken into account, the semi-realistic interactions describe the erosion of N = 20 and 28 magicity in the proton-deficient region, as well as the emergence of N = 16 and 32 magicity. In addition to the known magic numbers, possible magicity at N = 40, 56, 90, 124, 172, 178, 164, 184 and Z = 14, 16, 34, 38, 40, 58, 64, 92, 120, 124, 126 has been argued, in comparison with similar predictions obtained from the Gogny D1S and D1M interactions' (Nakada H. and Sugiura K., 2014, pp. 16).

Figure 16 and figure 17, are an alternative way to visualize the issues that were previously discussed. Figure 16 depicts the relationship between the proton number and the excitation energy E_{2+} which is plotted in a logarithmic scale. It can be easily inferred that there

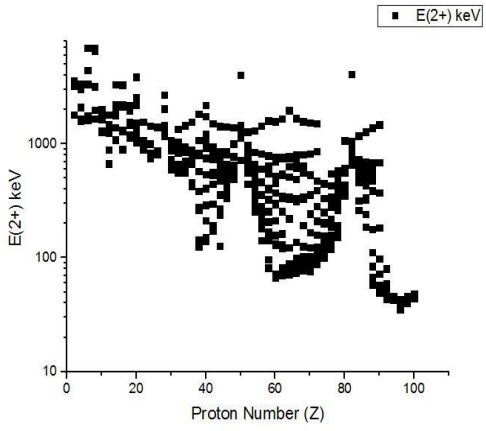

Figure 16. 2^+ Yrast Excitation Energies against Z

is a gradual decrease in the value of the excitation energy the greater the atomic number of the nuclides becomes, excluding, of course, the spikes corresponding to stable nuclides (classically, these should decrease as $A^{5/3}$ for the same deformation). Nevertheless, spikes at 8, 20, 28, 50, 82, and 126 (representing proton shell closures) can clearly be seen by the areas labelled on the graph. On the other hand, figure 17 illustrates the relationship between the excitation energy E_{2+} and the neutron number of the respective nuclides. The same conclusions can be reached as in the previous graph. In both cases, it is clear that the spikes correspond to the magic and doubly magic numbers.

However, figure 18 is furthermore demonstrating the collective effect of atomic mass number on the excitation of the respective nuclides. The two spikes, as discussed earlier, at the right side of the graph correspond to the doubly magic nuclides. On the other hand, there is a clear evidence for the shell structure model provided by the shell closures at N = 50, N = 82, and

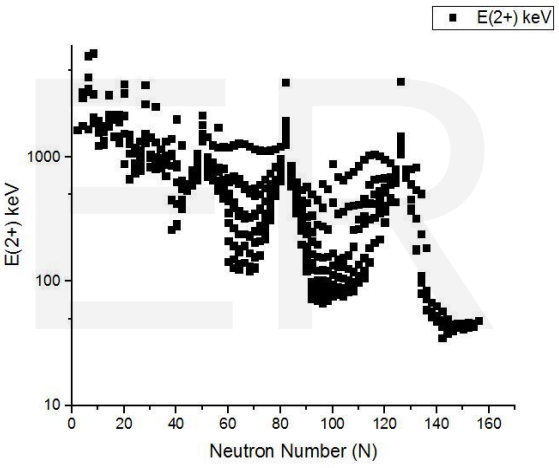

Figure 17. 2+ Yrast Excitation Energies of the 2+ state against N.

N = 126. The rest of these shell closures, namely at 8, 20, and 28 can also been seen, but for means keeping the graph simple they have not been indicated. It should be noted that there are two rather unexpected spikes at the region surrounding the ^{68}Ni (28 protons and 40 neutrons) and at the region surrounding the ^{90}Zr (40 protons and 50 neutrons). However, the first one has ~2.2 MeV excitation energy, while the analogous neutron intruder states in ^{90}Zr reside at 4126 keV and 5441 keV. This difference in the excitation energy can be explained by the shell model description of 0^+ intruder states. This model states that the excitation energies (and the respective differentiation of these nuclides as compared to the others) of both ^{68}Ni and ^{90}Zr can be explained by the fact that 'they are similar in spite of the difference in the unperturbed single-particle

shell-gap energies, as it is compensated to a large extent by the difference in pairing energies'(Pauwels D. et al, 2010). Furthermore, this highlights the fact that the stronger pair neutron scattering in ^{68}Ni triggers more active valence neutrons that highly interact with proton excitations around the region of $Z = 28$.

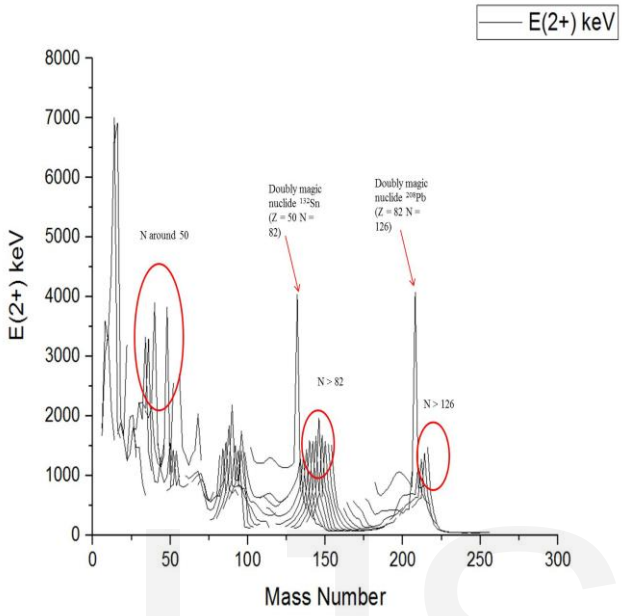

Figure 18. 2+Yrast excitation energies against the atomic mass. Two doubly magic nuclides are shown to have large spikes.

Hence, neutron pair scattering around $N = 40$ is far more important and influential than proton pair scattering around $Z = 40$. ^{132}Sn

3.2.Yrast 4^+ energies of even even nuclides

Figure 19 exhibits the excitation energy E_{4+} as a function of both the proton and neutron number. As expected, the average excitation energy is higher as compared to the respective E_{2+}; however, both plots appear to have a very similar shape. Hence, it can be concluded that the shell closures will be the same (same positions on the graph) regardless of which energy is plotted. An interesting fact is the great amount of energy that is needed at 6 neutrons or protons, despite the fact that this number is not a magic or doubly magic one.

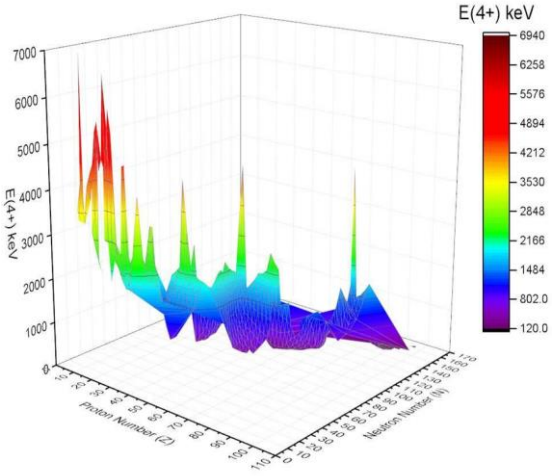

Figure 19. 4+Yrast excitation energies against N and Z

These results become more evident in the next figure where the collective effect of atomic mass number on the excitation E_{4+} of the respective nuclides. Once again this graph proves the existence of closed shell closures at the so-called magic number (2, 8, 20, 28, 50, 82, and 126). Moreover, the differences in the respective excitation energies for nuclides that have the same magic number of neutrons but not the same number of protons can be once again explained by the shell-model description as earlier.

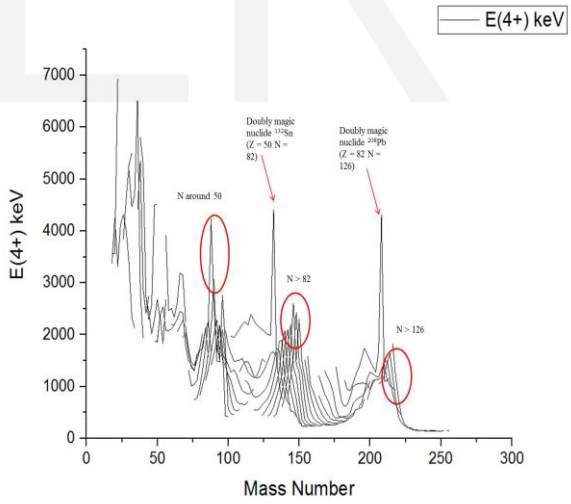

Figure 20. 4+ Yrast excitation energies for the 4^+ state in even-even nuclei against the atomic mass. Two doubly magic nuclides are shown to have large spikes

3.3.The R(E(4^+)/ E(2^+)) ratio

Interesting conclusions can be inferred by plotting the ratio of the two excitation energies (E(4^+)/ E(2^+)) as a function of both the proton and neutron number

of the nuclides. It is shown that there is a clear correlation between both excitation energies and that their respective ratio increases with the addition of valence nucleons until a maximum value is reached (that is found to be approximately 3.33). Following this value, the ratio tends to return back towards stability. It should be mentioned that the theoretical approach defines that this ratio should have a value of R = 3.333 for a near-perfect axially symmetric deformed rotor, whereas it should take values of R = 2.0 for idealized vibrational nuclei (perfect harmonic vibrators) (Alkhomashi N., 2010). On the other hand, the ratio of these two excitation energies for nuclei that have near closed shells (near magical nuclei) tend to take values that are less than 2.0. Moreover, figure 21 additionally shows that the larger the mass the lower the excitation energy is required in order to deform the nucleus. This suggests that heavier nuclei are more prone (and more easily) to

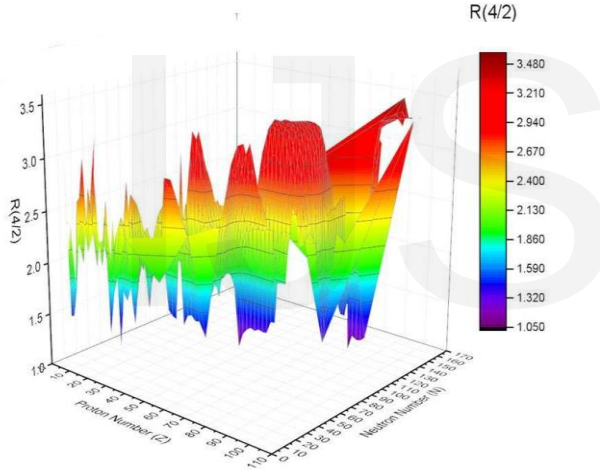

Figure 21. Plot of R(4/ 2), a measure of the ratio of the $E(4^+)$ energy to the $E(2^+)$ energy, against N and Z

deformation Of course, the exceptions in the region of high mass include the magic and doubly magic numbers. For instance, for tin and lead the ratio is expected (and is furthermore shown) to have lower values (R > 2.0) which correspond to spherical nuclei. The same conclusion can also be reached by plotting the ratio of the two excitation energies ($E(4^+)$ / $E(2^+)$) as a function of the atomic mass (figure 22). This graph is very useful because it directly exhibits the plethora of nuclei that are unstable and, thus easily deformed. For instance, and for the area that has atomic masses beyond 220, there are a large number of nuclei that are deformed. The same observation can be made for nuclides having

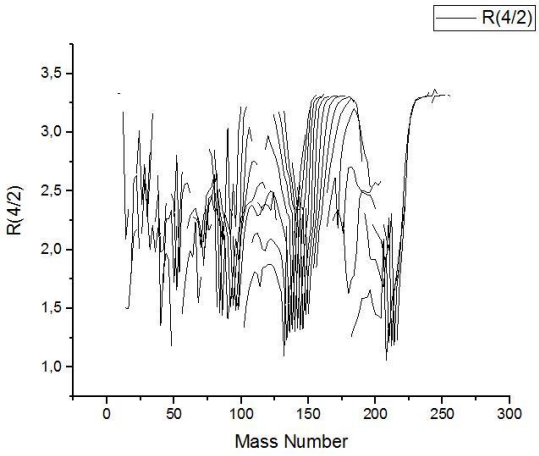

Figure 22. The ratio of $(E(4^+)/ E(2^+)$ against the atomic mass

atomic masses around the area of A = 150 and for light nuclei (A < 20).

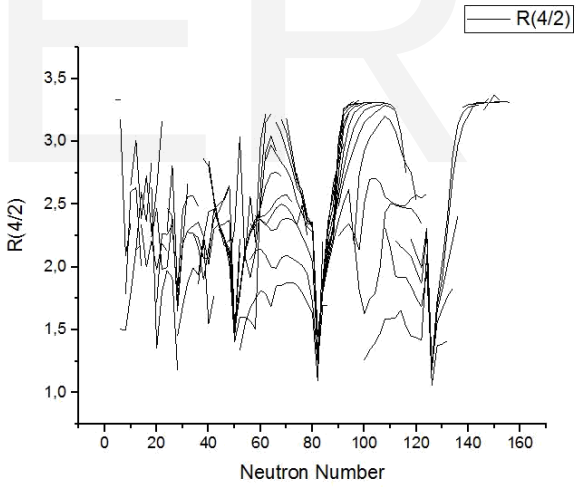

Figure 23. The ratio of $(E(4^+)/ E(2^+)$ against the neutron number

Figure 23 is demonstrating the ratio of the two excitation energies $(E(4^+)/ E(2^+)$ as a function of the neutron number. The magic numbers of 82 and 126 are now far more evident (R << 2.0).

3.4. Deformed nuclei

An additional parameter that can significantly aid in the quantification of nuclear deformation and the subsequent evaluation of the nuclides' nuclear

structure is the respective moment of inertia in the respective nuclei. This parameter can be calculated from eq. 8 and figure 13 and it demonstrates its independence from the given elements. Figure 24 exhibits the value of the moment of inertia against the proton and neutron number of the nuclides (figure 24). It is clearly shown that there is great variability regarding the value of the moment of inertia that can reach up to one order of magnitude. This is directly attributed to the respective nuclear shell structures but also to the number of valence nucleons that was previously discussed.

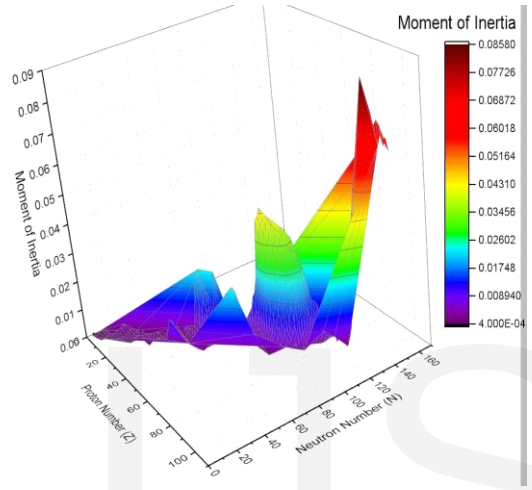

Figure 24. Moment of inertia for E_{2+} plotted against the number of protons and the number of neutrons

Furthermore, it can be deducted that regions which correspond to stable nuclides, such as the one located between the deformed rare earth and actinide elements (190 < A < 220) will show the lowest value for the moment of inertia. Hence, moment of inertia is a parameter that does not depend on the element itself but solely to the mass number (the greater the mass number the greater the value of inertia, except of course when it comes to the magic or doubly magic numbers).

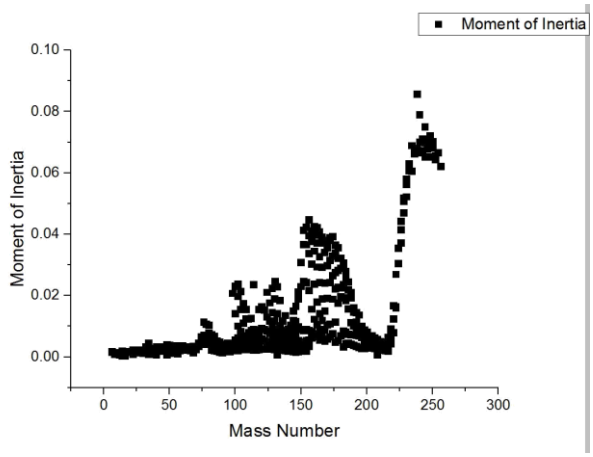

Figure 25. Moment of inertia for E_{2+} plotted against the atomic mass number, A.

Figure 25 also illustrates how the deformation parameter β varies with the respective nuclide masses. The $A^{5/3}$ dependence for collective nuclei is evident and it is shown at both figure 26 and figure 27. Indeed, these figures show that the moment of inertia of a nucleus does not depend upon which element it is, but also that this value is affected when the mass increases.

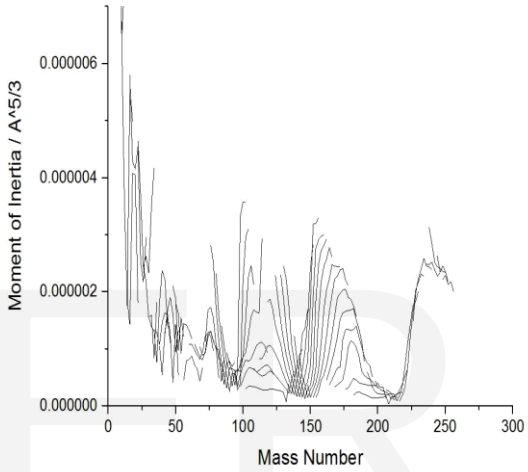

Figure 26. Moment of Inertia over the entire range as function of mass, A. Moment of inertia has been divided by $A^{5/3}$.

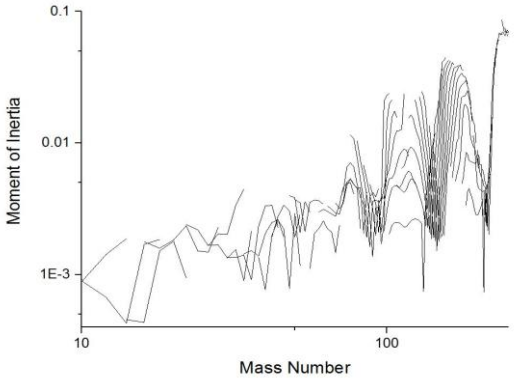

Figure 27. Log-log plot of moment of inertia and mass number showing the approximate $A^{5/3}$ dependence.

Finally, figure 26 demonstrates once again that the ration between the two Yrast energies ($4^+/2^+$) tends towards 3.33but cannot be greater. At this maximum value of 3.33 there is a wide range of potential nuclear deformations that can take place.

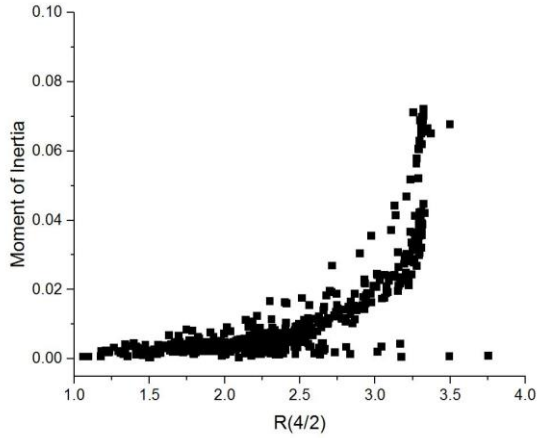

Figure 28: The nuclear deformation shown against the $E(4^+)/E(2^+)$ ratio. This shows the deviation of deformation for a perfect rotor. Two tracks show the observed classes of nuclear phase transitions.

3.5. Valence Product

An additional technique that can distinctly show and present indications of nuclear structure is the valence correction scheme (VCS). This technique is extremely useful because the huge array of data involved can sometimes obscure (or better said not clearly depict) the results that we want to present. VCS is a way of displaying the results in terms of the valence nucleons and the particular technique that will be used is the Np.Nn valence product parameter. This parameter simply denotes the product of the valence protons and valence neutrons or the product of the number of holes past mid-shell (in cases where the respective nucleon numbers are closer to the next filled (full) shell). Hence, it is extremely useful to show our results utilizing this parameter which essentially illustrates the trend as 'distance' from the magic numbers e.g. when Np.Nn is at a maximum value the nucleus is at its most unstable. It should be noted that this product Np.Nn can be thought of as presenting the strength of the respective interactions between the nucleons and it is the dominating factor regarding not only phase transitions but also regarding nuclear deformations. Figure 27 shows that as the product Np.Nn increases so does the deformation parameter (initially). However, and following the value of 200 the previous linear trend begins to change which directly reflects the addition of more and more valence nucleons (the so-called saturation region). Hamamoto was the first to point out that the square roots of the ratios of the measured and the single particle B (E2) values were proportional to the product Np.Nn (Hamamoto I., 1965).

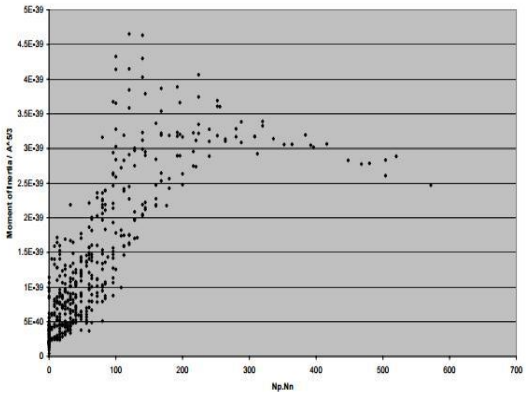

Figure 27. The variation of the deformation constant as a function of the Nn.Np valence product for the 2^+ yrast level.

The valence product appears to be higher the further away we go from the so - called magic numbers. This confirms that a high ratio will be found at the center of shells and, therefore this is the location where we are most likely to find the perfectly rotating deformed nuclei. On the other hand, the value of this product tends to zero if either the number of protons or number of neutrons coincides with a magic number.

4. Conclusions

All things considered, this dissertation presented a distinct and detailed analysis regarding the quantification of nuclear deformation and masses. The data of the 2^+ and 4^+ yrast energy states (Yrast states), the nuclear excited state energies of even □ even nuclei (nuclei with even number of protons and even number of neutrons) were collected from the literature and they were consequently plotted as a function of the respective proton and neutron numbers. Our results show that the shell structure model can be considered to be a reliable means in terms of describing the stability of nuclides. In fact, there appear to be certain magic numbers that which represent full cells and they are, thus very stable. This stability can be profoundly understood from figures 16 □24, where the excitation energy of the lowest excited state of most even □even nuclides

(the 2^+ state) is particularly high (spikes) at the magic numbers 2, 8, 20, 28, 50, 82, and 126 (or doubly magic isotopes with both proton and neutron numbers matching the magic ones) and, hence correspond to full shells. The two spikes, as discussed earlier, at the right side of the graph of figure 18 correspond to the doubly magic nuclides. Moreover, it can also be inferred that the heavier a nucleus is the lower excitation energy it possesses (high deformation areas). Nevertheless, an additional issue that was examined was the relative difference that was presented with respect to neutron pair scattering and proton pair scattering. The underline incentive for this issue was the discovery of two rather unexpected spikes at the region surrounding the ^{68}Ni (28 protons and 40 neutrons) and at the region surrounding the ^{90}Zr (40 protons and 50 neutrons). Their respective difference in excitation energies can be explained by the shell model description of 0^+ intruder states and proves that neutron pair scattering around $N = 40$ is far more important and influential than proton pair scattering around $Z = 40$.

The excitation energy data of the 2^+ and 4^+ states, the ratio $E(4^+) / E(2^+)$ was found. This ratio takes values within the range of $1.5 \rightarrow 3.33$ and it is a clear indication of the nuclear deformity of each and every nucleus. It was shown that this ratio reaches a value of $R = 3.333$ for a near - perfect axially symmetric deformed rotor, whereas it takes values of $R = 2.0$ for idealized vibrational nuclei (perfect harmonic vibrators). However, and as opposed to these values, the ratio of these two excitation energies for nuclei that have near closed shells (near magical nuclei) tend to take values that are less than 2.0. Once again the high instability of heavier nuclei is demonstrated (figure 21). Furthermore, the moment of inertia was also examined (figure 24) and it was found that regions which correspond to stable nuclides, such as the one located between the deformed rare earth and actinid elements ($190 < A < 220$), will show the lowest value for the moment of inertia. It should be also stated that these values show a great degree of variability (up to one order of magnitude), an issue that can be explained by the nuclear shell structure and to the number of valence nucleons. The moment of inertia is approximately proportional to $A^{5/3}$, therefore, when this value is divided by this dependence the result is a deformation constant that can be also utilized in order to define the eccentricity of the ellipsoid nuclides. It has also been shown that for $Nn.Np$ values greater than 200 this deformation is greatest but also becomes saturated. This practically suggests the fact that in cases where a large number of valence nucleons is present in the respective nuclear structure then there is a collective excitation that triggers the nuclei to be deformed. Finally, the deformation parameter showed maxima at specific regions in the nuclear chart which can be seen in figure 25. The valence product appears to be higher the further away we go from the so-called magic numbers. Hence, deformation is once again shown that it is directly dependent to the number of valence nucleons.

References

ABADI VAHID MM. ET AL. 2015. Study of Nuclear Shell Model Open Science Journal of Modern Physics, 2, pp. 19-22.

ALDER K. ET AL 1956. Review of Modern Physics. 18.

ALKHOMASHI N. 2010. Beta Decay Studies of Heavy Neutron-Rich Nuclei Around A=190. Department of Physics, School of Electronics and Physical Sciences, University of Surrey,.

BEHRENS T. 2009. The Evolution of B(E2) Values Around the Doubly-Magic Nucleus 132Sn. Fakultat fur Physik der Technischen Universitat Munchen Physik-Department E12.

BLAUM K. ET AL 2013. Precision Atomic Physics Techniques for Nuclear Physics with Radioactive Beams. Phys. Scr., 2013.

BOHR A. & MOTTELSON B. 1955. MOMENTS OF INERTIA OF ROTATING NUCLE I. Det Kongelige Danske Videnskabernes Selska b Matematisk-fysiske Meddelelser, 30, 1-24.

BOWLER MG. 1973. Nuclear Physics: International Series of Monographs in Natural Philosophy. Pergamon Press Ltd Headington Hill Hall, Oxford, UK.

BROWN GE. ET AL 2010. The Nucleon-nucleon Interaction and the Nuclear Many-body Problem. World Scientific Publishment Co. Pte. Ltd Singapore.

BRYAN J. 2013. Introduction to Nuclear Science, Second Edition. Taylor & Francis Group Florida.

CAMPBELL MK. & GOLDSTEIN N. 2012. Discovering Atoms. The Rosen Publishing Group, New York.

CASTEN R. 2000. Nuclear Structure from a Simple Perspective. Oxford University Press.

CASTEN RF. 1985. Phys. Rev. Lett, 54, 1991.

CDFE.SINP.MSU.RU Chart of nucleus shape and size parameters. http://cdfe.sinp.msu.ru/services/radchart/radhelp.html (accessed online on 2nd August 2015).

CYBERPHYSICS.CO.UK 2015. Strong Nuclear Force. http://www.cyberphysics.co.uk/topics/particle/strong.html (accessed online on 3rd September 2015).

DE GRUYTER W. 1997. Constituents of matter: atoms, molecules, nuclei and particles. University of Michigan US.

DEMTRIJDER W. 2010. Atoms, Molecules and Photons: An Introduction to Atomic-, Molecular- and Quantum Physics. Springer Heidelberg.

DURRANT A. 2000. Quantum Physics of Matter. Open University, Walton Hall UK.

HAMAMOTO I. 1965. Nucl. Phys, 73.

HATSUDA T. 2011, pp. 1. Lattice Nuclear Force. Festschrift for Gerry Brown, ed. Sabine Lee (World Scientific, Singapore).

HELLEM J. 2008. An Investigation into the 2+ and 4+ Excitation Energies and Nuclear Deformation Dissertation submitted to the Department of Physics, in partial fulfilment of the degree of Master of Radiation and Environmental Protection

HINKE CB. ET AL 2012. Superallowed Gamow Teller decay of the doubly magic nucleus 100Sn. Nature 486, pp. 341-345.

HOSSAIN I. ET AL 2014. B(E2) value of even-even 108-112Pd isotopes by interacting boson model-1. Chinese Physics C, 38.

HYPERPHYSICS.PHY-ASTR.GSU.EDU 2015. Shell Model of Nucleus. http://hyperphysics.phy-astr.gsu.edu/hbase/nuclear/shell.html (accessed online on 2 August 2015).

IFM.LIU.SE 2015. Liquid-Drop Model and the Semiempirical Mass Formula. https://people.ifm.liu.se/boman/kvantfysik_larare/Liquid.pdf (accessed online on 2 August 2015).

JELLEY NA. 2007. Fundamentals of nuclear physics. Cambridge University Press. JEVREMOVIC T. 2009. Nuclear Principles in Engineering. Springer Science, +Business Media LLC, USA.

KAKANI SL. 2006. Material Science. New Age International Ltd Publishers.

KHAGRAM P. 2007. Investigating the properties and deformation of the nucleus by considering the E(2+) and E(4+) excited energy states of even-even nuclei Faculty of Engineering and Physical Sciences The University of Surrey Guildford.

KRANE KS. 1998. Introductory Nuclear Physics. Wiley Blackwell Ltd, West Sussex UK. LILLEY J. 2001. Nuclear Physics, Principle and Applications. Wiley Blackwell Ltd, West Sussex UK.

LILLEY J. 2002. Nuclear Physics (Principles and Applications). ISBN 0471979368(paper) ISBN 04719735(cased).

LONGO L. 2015. Lifetime measurements of excited states in nuclei around the doubly-magic 48Ca and 208P b. Dipartimento di Fisica e Astronomia "Galileo Galilei" Laurea Triennale in Fisica.

42

MAGILL J. & GALY J. 2005. Radioactivity Radionuclides Radiation. Springer Berlin. MARTIN B. 2011. Nuclear and Particle Physics: An Introduction. Wiley Blackwell Ltd, West Sussex UK.

MASON TE. ET AL 2013. The early development of neutron diffraction: science in the wings of the Manhattan Project. Acta Cryst, 69, pp. 37-44.

MICHIMASA S. ET AL 2014. Phys. Rev. C, 89.

MOODY KJ. ET AL 2005. Nuclear Forensic Analysis. Taylor and Francis Group LLC. NAKADA H. & SUGIURA K. 2014, pp. 16. Predicting magic numbers of nuclei with semi-

realistic nucleon□nucleon interactions. *Prog. Theor. Exp. Phys.*, 33.

NAKATSUKASA T. 2012. Density functional approaches to collective phenomena in nuclei: Time-dependent density functional theory for perturbative and non-perturbative nuclear dynamics. *Prog. Theor. Exp. Phys.*

NEERAJ M. 2011. Applied Physics for Engineers. *PHI Learning Private, India.*

NIAZ M. 2009. Critical Appraisal of Physical Science as a Human Enterprise. *Springer Science, Venezuela.*

NNDC.BNL.GOV 2015. National Nuclear Data Center. http://www.nndc.bnl.gov/ (accessed online on 2nd August 2015).

OLMSTED J. & WILLIAMS GM. 1997. Chemistry: The Molecular Science. *WM. C. Brown Publishers, USA.*

OVENDEN C. An Investigation into the 2+ and 4+ Excitation Energies and Nuclear Deformation (PHR1).

PATEL SB. 2006. Nuclear Physics: An Introduction, reprint. *New Age International Ltd Publishers.*

PAUWELS D. ET AL 2010. Pairing-excitation versus intruder states in 68Ni and 90Zr. *Phys.Rev.C*, 82.

PEARSON J. 2008. Nuclear Physics. http://www.joffline.com/physics_docs/y3s6/nuclearphysics_ln.pdf (accessed online on 3rd September 2015).

PHYSICSWORLD.COM 2011. A taste of the exotic. http://physicsworld.com/cws/article/print/2011/nov/03/a-taste-of-the-exotic (accessed online on 2nd Augist 2015).

RAMAN S. ET AL. 2001. TRANSITION PROBABILITY FROM THE GROUND TO THE FIRST-EXCITED 2+ STATE OF EVEN□EVEN NUCLIDES. *Atomic Data and Nuclear Data Tables*, 78, pp. 1-128.

REED BC. 2013. A Short History of Nuclear Physics to the Mid-1930s. *Springer.*

REGAN PH. ET AL. 2003. Signature for Vibrational to Rotational Evolution Along the Yrast Line. *Phys. Rev. Lett.*, 90.

RING P. & SCHUCK P. 1980. The Nuclear Many-Body Problem. *Springer, Berlin, 1980.* RODRIGUEZ-GUZMAN, R., ROBLEDO, L. M. & SHARMA, M. M. 2015. Microscopic description of quadrupole collectivity in neutron-rich nuclei across the N = 126 shell closure. *The European Physical Journal A*, 51, pp. 1-17.

ROWE D. & WOOD J. 2010. Fundamentals of Nuclear Models: Foundational Models. *World Scientific Publishment Co. Pte. Ltd Singapore.*

RYDIN R. 2011. A new approach to finding magic numbers for heavy and superheavy elements. *Annals of Nuclear Energy*, 38, pp. 238-242.

SHEF.AC.UK 2003. Fission, fusion and the bomb. http://physics-database.group.shef.ac.uk/phy303/phy303-6.html (accessed online on 2nd August 2015).

STOCK R. 2006. Encyclopedia of Nuclear Physics and its Applications. *Universitat Frankfurt, Wiley-VCH.*

TRENTALAGE S. & KOONIN E. 1980. Shape parametrisation for liquid drop studies. *Physical Review C*, 22, 1159-1167.

UNI-KOELN.DE 2015. Collective properties of even-even nuclei. https://www.ikp.uni-

koeln.de/students/casten/day4lecture2.pdf (accessed online on 2 august 2015).

VAN DOMMELEN L. 2013. Quantum Mechanics for Engineers. https://www.eng.fsu.edu/~dommelen/quantum/style_a/ntcs.html#SECTION086132000 000000000000 (accessed online on 2nd August 2015).

VAN OERS WTH. 1992. Intersections Between Particle and Nuclear Physics. American Institute of Physics, University of California.

WALKER J. 2004. A short history of the knowledge of the atom. http://www.nobeliefs.com/atom.htm (accessed online on August 2 2015).

WALTHER J. 2009. Essentials of Geochemistry. Jones and Bartlett Learning publishers LLC.

WEB.UTK.EDU 2013. http://web.utk.edu/~kamyshko/P232/Chapter%2043.pdf September 2015).

WINN W. 2010. Introduction to Understandable Physics: Modern and Frontier Physics. AuthorHouse, USA.

YARWOOD J. 1973. Atomic and Nuclear Physics. ISBN 072310607X, , pp. 428 - 429.

Appendix I.

Nuclide	Proton Number (Z)	Neutron Number (N)	Mass Number	E(2+) keV	E(4+) keV	R(4/2)
$^{4}_{2}He_{2}$	2	2	4,002603254			
$^{6}_{2}He_{4}$	2	4	6,0188891	1797		
$^{8}_{2}He_{6}$	2	6	8,033922	3590		
$^{10}_{2}He_{8}$	2	8	10,0524	3240		
$^{6}_{4}Be_{2}$	4	2	6,019726	1670		
$^{8}_{4}Be_{4}$	4	4	8,0053051	3040	1,14E+04	3,75E+00
$^{10}_{4}Be_{6}$	4	6	10,013533	3368,03	11760	3,49E+00
$^{12}_{4}Be_{8}$	4	8	12,026921	2102		
$^{14}_{4}Be_{10}$	4	10	14,04289	1590		
$^{10}_{6}C_{4}$	6	4	10,0168532	3353,6		

$^{12}_{6}C_{6}$	6	6	12	4438,91	14083	3,17E+00
$^{14}_{6}C_{8}$	6	8	14,00324199	7012	14667	2,09E+00
$^{16}_{6}C_{10}$	6	10	16,014701	1766	4142	2,35E+00
$^{18}_{6}C_{12}$	6	12	18,02676	1620		
$^{14}_{8}O_{6}$	8	6	14,00859625	6590	9915	1,50E+00
$^{16}_{8}O_{8}$	8	8	15,99491462	6917,1	10356	1,50E+00
$^{18}_{8}O_{10}$	8	10	17,999161	1982,1	3554,84	1,79E+00
$^{20}_{8}O_{12}$	8	12	20,0040767	1673,68	3570	2,13E+00
$^{22}_{8}O_{14}$	8	14	22,00997	3190	6936	2,17E+00
$^{16}_{10}Ne_{6}$	10	6	16,025761	1690		
$^{18}_{10}Ne_{8}$	10	8	18,0057082	1887,3	3376,2	1,79E+00
$^{20}_{10}Ne_{10}$	10	10	19,99244018	1633,674	4247,7	2,60E+00
$^{22}_{10}Ne_{12}$	10	12	21,99138511	1274,542	3357,7	2,63E+00
$^{24}_{10}Ne_{14}$	10	14	23,9936108	1981,6	3972	2,00E+00
$^{26}_{10}Ne_{16}$	10	16	26,000461	2018,2		
$^{28}_{10}Ne_{18}$	10	18	28,01207	1310	3010	2,30E+00
$^{22}_{12}Mg_{10}$	12	10	21,9995738	1246,3	3308,22	2,65E+00
$^{24}_{12}Mg_{12}$	12	12	23,9850417	1368,675	4122,889	3,01E+00
$^{26}_{12}Mg_{14}$	12	14	25,98259293	1808,73	4318,88	2,39E+00
$^{28}_{12}Mg_{16}$	12	16	27,9838768	1473,4	4021	2,73E+00
$^{30}_{12}Mg_{18}$	12	18	29,990434	1482,2	3381,2	2,28E+00
$^{32}_{12}Mg_{20}$	12	20	31,998975	885,5	2322,3	2,62E+00
$^{34}_{12}Mg_{22}$	12	22	34,00946	670	2120	3,16E+00

1 2 2						
^{26}Si 1 4 12	14	12	25,99233	1795,9	3842,2	2,14E+00
^{28}Si 1 4 14	14	14	27,97692653	1779,03	4617,86	2,60E+00
^{30}Si 1 4 16	14	16	29,97377017	2235,33	5279,37	2,36E+00
^{32}Si 1 4 18	14	18	31,97414808	1941,5	5502	2,83E+00
^{34}Si 1 4 20	14	20	33,978576	3327,5		
^{36}Si 1 4 22	14	22	35,9866	1399,25	2850	2,04E+00
^{38}Si 1 4 24	14	24	37,99563	1084,2		

46

$^{30}_{16}S_{14}$	16	14	29,984903	2210,6	5168	2,34E+00
$^{32}_{16}S_{16}$	16	16	31,972071	2230,3	4459,1	2,00E+00
$^{34}_{16}S_{18}$	16	18	33,9678669	2127,564	4698,88	2,21E+00
$^{36}_{16}S_{20}$	16	20	35,96708076	3290,9	6514,4	1,98E+00
$^{38}_{16}S_{22}$	16	22	37,971163	1292	2825,2	2,19E+00
$^{40}_{16}S_{24}$	16	24	39,97545	900	1916,84	2,13E+00
$^{42}_{16}S_{26}$	16	26	41,98102	890		
$^{44}_{16}S_{28}$	16	28	43,99021	1315	2457	1,87E+00
$^{34}_{18}Ar_{16}$	18	16	33,9802712	2090,9		
$^{36}_{18}Ar_{18}$	18	18	35,96754511	1970,39	4414,4	2,24E+00
$^{38}_{18}Ar_{20}$	18	20	37,9627324	2167,462	5349,4	2,47E+00
$^{40}_{18}Ar_{22}$	18	22	39,96238312	1460,859	2892,6	1,98E+00
$^{42}_{18}Ar_{24}$	18	24	41,963046	1208,2	2414	2,00E+00
$^{44}_{18}Ar_{26}$	18	26	43,964924	1144	2746,2	2,40E+00
$^{46}_{18}Ar_{28}$	18	28	45,96809	1550		
$^{38}_{20}Ca_{18}$	20	18	37,976318	2206	5810	2,63E+00
$^{40}_{20}Ca_{20}$	20	20	39,96259098	3904,38	5278,8	1,35E+00
$^{42}_{20}Ca_{22}$	20	22	41,95861801	1524,73	2752,41	1,81E+00
$^{44}_{20}Ca_{24}$	20	24	43,9554818	1157,047	2283,114	1,97E+00
$^{46}_{20}Ca_{26}$	20	26	45,9536926	1346	2574,7	1,91E+00
$^{48}_{20}Ca_{28}$	20	28	47,952534	3831,72	4503,14	1,18E+00
$^{50}_{20}Ca_{30}$	20	30	49,957519	1026	4515,02	4,40E+00
$^{52}_{20}Ca_{32}$	20	32	51,9651	2563		

$^{42}_{22}Ti_{20}$	22	20	41,973031	1554,9	2676,6	1,72E+00
$^{44}_{22}Ti_{22}$	22	22	43,9596901	1082,99	2452,33	2,26E+00
$^{46}_{22}Ti_{24}$	22	24	45,9526316	889,286	2009,846	2,26E+00
$^{48}_{22}Ti_{26}$	22	26	47,9479463	983,519	2295,654	2,33E+00
$^{50}_{22}Ti_{28}$	22	28	49,9447912	1553,778	2674,91	1,72E+00
$^{52}_{22}Ti_{30}$	22	30	51,946897	1049,73	2317,65	2,21E+00
$^{48}_{24}Cr_{24}$	24	24	47,954032	752,16	1858,47	2,47E+00
$^{50}_{24}Cr_{26}$	24	26	49,9460442	783,3	1881,31	2,40E+00
$^{52}_{24}Cr_{28}$	24	28	51,9405075	1434,09	2369,633	1,65E+00
$^{54}_{24}Cr_{30}$	24	30	53,9388804	834,855	1823,93	2,18E+00
$^{56}_{24}Cr_{32}$	24	32	55,9406531	1006,61	2681,7	2,66E+00
$^{50}_{26}Fe_{24}$	26	24	49,96299	810	1851,5	2,29E+00
$^{52}_{26}Fe_{26}$	26	26	51,948114	849,6	2384,55	2,81E+00
$^{54}_{26}Fe_{28}$	26	28	53,9396105	1408,19	2538,1	1,80E+00
$^{56}_{26}Fe_{30}$	26	30	55,9349375	846,776	2085,1045	2,46E+00
$^{58}_{26}Fe_{32}$	26	32	57,9332756	810,784	2076,52	2,56E+00
$^{60}_{26}Fe_{34}$	26	34	59,934072	823,63	2114,6	2,57E+00
$^{62}_{26}Fe_{36}$	26	36	61,936767	876,8	2176,47	2,48E+00
$^{56}_{28}Ni_{28}$	28	28	55,942132	2700,6	3923,6	1,45E+00
$^{58}_{28}Ni_{30}$	28	30	57,9353429	1454	2459,21	1,69E+00
$^{60}_{28}Ni_{32}$	28	32	59,9307864	1332,518	2505,753	1,88E+00
$^{62}_{28}Ni_{34}$	28	34	61,9283451	1172,91	2336,52	1,99E+00
$^{64}_{28}Ni_{36}$	28	36	63,927966	1345,75	2610,1	1,94E+00
$^{66}_{28}Ni_{38}$	28	38	65,9291393	1425,1	3185,44	2,24E+00
$^{68}_{28}Ni_{40}$	28	40	67,931869	2033,2	3149,2	1,55E+00
$^{70}_{28}Ni$	28	42	69,9365	1259,6	2229,5	1,77E+00

47, 42						

$^{60}_{30}Zn_{30}$	30	30	59,941827	1004,1	2193	2,18E+00
$^{62}_{30}Zn_{32}$	30	32	61,93433	954	2186,06	2,29E+00
$^{64}_{30}Zn_{34}$	30	34	63,9291422	991,55	2306,75	2,33E+00
$^{66}_{30}Zn_{36}$	30	36	65,9260334	1039,39	2451,01	2,36E+00
$^{68}_{30}Zn_{38}$	30	38	67,9248442	1077,37	2417,4	2,24E+00
$^{70}_{30}Zn_{40}$	30	40	69,9253193	884,8	1786,33	2,02E+00
$^{72}_{30}Zn_{42}$	30	42	71,926858	652,5	1499,52	2,30E+00
$^{74}_{30}Zn_{44}$	30	44	73,92946	605,82	1418,56	2,34E+00
$^{76}_{30}Zn_{46}$	30	46	75,93329	598,68	1296,46	2,17E+00
$^{78}_{30}Zn_{48}$	30	48	77,93844	729,6	1620,07	2,22E+00
$^{64}_{32}Ge_{32}$	32	32	63,94165	901,7	2052,6	2,28E+00
$^{66}_{32}Ge_{34}$	32	34	65,93384	957	2173,29	2,27E+00
$^{68}_{32}Ge_{36}$	32	36	67,928094	1015,99	2267,83	2,23E+00
$^{70}_{32}Ge_{38}$	32	38	69,9242474	1039,25	2153,16	2,07E+00
$^{72}_{32}Ge_{40}$	32	40	71,9220758	834,011	1728,3	2,07E+00
$^{74}_{32}Ge_{42}$	32	42	73,9211778	595,85	1463,759	2,46E+00
$^{76}_{32}Ge_{44}$	32	44	75,9214026	562,93	1410,08	2,50E+00
$^{78}_{32}Ge_{46}$	32	46	77,922853	619,34	1570,2	2,54E+00
$^{80}_{32}Ge_{48}$	32	48	79,92537	659,15	1742,59	2,64E+00
$^{82}_{32}Ge_{50}$	32	50	81,92955	1348,04	2028,6	1,50E+00
$^{68}_{34}Se_{34}$	34	34	67,9418	854,2	1942,1	2,27E+00
$^{70}_{34}Se_{36}$	34	36	69,93339	944,6	2038,1	2,16E+00
$^{72}_{34}Se_{38}$	34	38	71,927112	862,08	1636,86	1,90E+00
$^{74}_{34}Se_{40}$	34	40	73,9224764	634,75	1363,17	2,15E+00
$^{76}_{34}Se_{42}$	34	42	75,9192136	559,102	1330,86	2,38E+00
$^{78}_{34}Se_{44}$	34	44	77,9173091	613,727	1502,825	2,45E+00
$^{80}_{34}Se_{46}$	34	46	79,9165213	666,16	1701,45	2,55E+00
$^{82}_{34}Se_{48}$	34	48	81,9166994	654,69	1735,12	2,65E+00
$^{84}_{34}Se_{50}$	34	50	83,918462	1454,42	2121,65	1,46E+00

34 50						
34 52	Se	34	52	85,924272	704,1	1567,9	2,23E+00
36 36	Kr	36	36	71,942092	709,1	1321,4	1,86E+00
36 38	Kr	36	38	73,9330844	455,8	1013,32	2,22E+00
36 40	Kr	36	40	75,92591	423,96	1034,62	2,44E+00
36 42	Kr	36	42	77,9203648	455,04	1119,48	2,46E+00
36 44	Kr	46	44	79,916379	616,61	1436,09	2,33E+00
36 46	Kr	36	46	81,9134836	776,521	1820,53	2,34E+00
36 48	Kr	36	48	83,911507	881,615	2095	2,38E+00
36 50	Kr	36	50	85,91061073	1564,87	2250	1,44E+00
36 52	Kr	36	52	87,914447	775,31	1643,78	2,12E+00
36 54	Kr	36	54	89,919517	707,13		
36 56	Kr	36	56	91,926156	769	1804	2,35E+00
36 58	Kr	36	58	93,93436	665	1518,7	2,28E+00

76 Sr 38 38	38	38	75,94177	260,9	746,7	2,86E+00
78 Sr 38 40	38	40	77,93218	278,5	780,8	2,80E+00
80 Sr 38 42	38	42	79,924521	385,86	980,68	2,54E+00
82 Sr 38 44	38	44	81,918402	573,54	1328,54	2,32E+00
84 Sr 38 46	38	46	83,913425	793,3	1767,69	2,23E+00
86 Sr 38 48	38	48	85,90926073	1076,68	2229,81	2,07E+00
88 Sr 38 50	38	50	87,90561226	1836,087	4232	2,30E+00
90 Sr 38 52	38	52	89,907738	831,68	2527,92	3,04E+00
92 Sr 38 54	38	54	91,911038	814,98	1673,3	2,05E+00
94 Sr 38 56	38	56	93,915361	836,91	2146	2,56E+00
96 Sr 38 58	38	58	95,921697	814,93	1792,77	2,20E+00
98 Sr 38 60	38	60	97,928453	144,225	433,52	3,01E+00
100 Sr 38 62	38	62	99,93535	129,7	417,98	3,22E+00
102 Sr 38 64	38	64	101,94302	126		
80 Zr 40 40	40	40	79,9404	289,9	825,8	2,85E+00
82 Zr 40 42	40	42	81,93109	407,3	1040,84	2,56E+00
84 Zr 40 44	40	44	83,92325	540	1261,81	2,34E+00
86 Zr	40	46	85,91647	751,75	1666,57	2,22E+00

96 Zr 40 56	40	56	95,9082734	1750,498	2750	1,57E+00
98 Zr 40 58	40	58	97,912735	1222,93	1843,45	1,51E+00
100 Zr 40 60	40	60	99,91776	212,53	564,486	2,66E+00
102 Zr 40 62	40	62	101,92298	151,77	478,28	3,15E+00
104 Zr 40 64	40	64	103,92878	140,3	452,1	3,22E+00
84 Mo 42 42	42	42	83,94009	443,8	1117,3	2,52E+00
86 Mo 42 44	42	44	85,9307	566,6	1327,5	2,34E+00
88 Mo 42 46	42	46	87,921953	740,53	1654,83	2,23E+00
90 Mo 42 48	42	48	89,913937	947,97	2002,06	2,11E+00
92 Mo 42 50	42	50	91,906811	1509,49	2282,61	1,51E+00
94 Mo 42 52	42	52	93,9050883	871,096	1573,76	1,81E+00
96 Mo 42 54	42	54	95,9046795	778,245	1628,188	2,09E+00
98 Mo 42 56	42	56	97,9054082	787,384	1510,039	1,92E+00
100 Mo 42 58	42	58	99,907477	535,57	1136,09	2,12E+00
102 Mo	42	60	101,910297	296,597	743,73	2,51E+00

$^{4}_{2}$ $^{6}_{0}$						
$^{104}_{42}Mo_{62}$	42	62	103,91376	192,3	560,68	2,92E+00
$^{4}_{2}$ $^{6}_{2}$						
$^{106}_{42}Mo_{64}$	42	64	105,918137	171,548	522,32	3,04E+00
$^{4}_{2}$ $^{6}_{4}$						
$^{108}_{42}Mo_{66}$	42	66	107,92345	192,9	563,69	2,92E+00
$^{4}_{2}$ $^{6}_{6}$						
$^{8}_{4}$ $^{8}_{4}$ $^{Ru}_{4}$44	44	44	87,94026	616	1416	2,30E+00
$^{9}_{4}$ $^{0}_{4}$ Ru_{46}	44	46	89,92989	738,1	1638,11	2,22E+00
$^{9}_{4}$ $^{2}_{4}$ Ru_{48}	44	48	91,92012	864,6	1854,9	2,15E+00
$^{9}_{4}$ $^{4}_{4}$ Ru 50	44	50	93,91136	1430,51	2186,6	1,53E+00
$^{9}_{4}$ $^{6}_{4}$ Ru 52	44	52	95,907598	832,57	1518,05	1,82E+00
$^{9}_{4}$ $^{8}_{4}$ Ru 54	44	54	97,905287	652,44	1397,82	2,14E+00
$^{100}_{44}$ $^{Ru}_{4}$ $^{5}_{6}$	44	56	99,9042195	539,506	1226,465	2,27E+00
$^{102}_{44}$ $^{Ru}_{4}$ $^{5}_{8}$	44	58	101,9043493	475,079	1106,43	2,33E+00
$^{104}_{44}Ru_{60}$	44	60	103,905433	358,02	888,48	2,48E+00
$^{106}_{44}$ $^{Ru}_{4}$ $^{6}_{2}$	44	62	105,907329	270,07	714,69	2,65E+00

49

$^{108}_{44}Ru_{64}$	44	64	107,91017	242,24	665,1	2,75E+00
$^{110}_{44}Ru_{66}$	44	66	109,91414	240,71	663,35	2,76E+00
$^{112}_{44}Ru_{68}$	44	68	111,91897	236,66	644,97	2,73E+00
$^{114}_{44}Ru_{70}$	44	70	113,92428	127	708,2	5,58E+00
$^{94}_{46}Pd_{48}$	46	48	93,92877	814	1719,11	2,11E+00
$^{96}_{46}Pd_{50}$	46	50	95,91816	1415,4	2099,01	1,48E+00
$^{98}_{46}Pd_{52}$	46	52	97,912721	863,1	1541,4	1,79E+00
$^{100}_{46}Pd_{54}$	46	54	99,908506	665,56	1416,15	2,13E+00
$^{102}_{46}Pd_{56}$	46	56	101,905609	556,43	1275,91	2,29E+00
$^{104}_{46}Pd_{58}$	46	58	103,904036	555,81	1323,59	2,38E+00
$^{106}_{46}Pd_{60}$	46	60	105,903486	511,851	1229,3	2,40E+00
$^{108}_{46}Pd_{62}$	46	62	107,903892	433,938	1048,216	2,42E+00
$^{110}_{46}Pd_{64}$	46	64	109,905153	373,81	920,78	2,46E+00
$^{112}_{46}Pd_{66}$	46	66	111,907314	348,79	882,96	2,53E+00
$^{114}_{46}Pd_{68}$	46	68	113,910363	332,5	852,37	2,56E+00
$^{116}_{46}Pd_{70}$	46	70	115,91416	340,6	877,58	2,58E+00
$^{118}_{46}Pd_{72}$	46	72	117,91898	378,4	953,2	2,52E+00
$^{98}_{48}Cd_{50}$	48	50	97,9274	1394,7	2082,3	1,49E+00
$^{100}_{48}Cd_{52}$	48	52	99,92029	1004,5	1799	1,79E+00
$^{102}_{48}Cd_{54}$	48	54	101,91446	776,55	1637,9	2,11E+00
$^{104}_{48}Cd_{56}$	48	56	103,909849	658	1492,1	2,27E+00
$^{106}_{48}Cd_{58}$	48	58	105,906459	632,64	1493,78	2,36E+00
$^{108}_{48}Cd_{60}$	48	60	107,904184	632,986	1508,466	2,38E+00
$^{110}_{48}Cd_{62}$	48	62	109,9030021	657,7638	1542,44	2,34E+00
$^{112}_{48}Cd_{64}$	48	64	111,9027578	617,52	1415,48	2,29E+00

$^{114}_{48}Cd_{66}$	48	66	113,9033585	558,456	1283,789	2,30E+00
$^{116}_{48}Cd_{68}$	48	68	115,904756	513,49	1219,45	2,37E+00
$^{118}_{48}Cd_{70}$	48	70	117,906915	487,77	1164,94	2,39E+00
$^{120}_{48}Cd_{72}$	48	72	119,90985	505,9	1203,7	2,38E+00
$^{122}_{48}Cd_{74}$	48	74	121,91333	569,45	1329,15	2,33E+00
$^{124}_{48}Cd_{76}$	48	76	123,91765	613,33	1530	2,49E+00
$^{126}_{48}Cd_{78}$	48	78	125,92235	652	1467	2,25E+00
$^{102}_{50}Sn_{52}$	50	52	101,9303	1472	1969	1,34E+00
$^{104}_{50}Sn_{54}$	50	54	103,92314	1260,1	1942,7	1,54E+00
$^{106}_{50}Sn_{56}$	50	56	105,91688	1207,7	2019,6	1,67E+00
$^{108}_{50}Sn_{58}$	50	58	107,911925	1206,07	2111,11	1,75E+00
$^{110}_{50}Sn_{60}$	50	60	109,907843	1211,89	2197,05	1,81E+00
$^{112}_{50}Sn_{62}$	50	62	111,904818	1256,85	2247,39	1,79E+00
$^{114}_{50}Sn_{64}$	50	64	113,902779	1299,92	2187,602	1,68E+00
$^{116}_{50}Sn_{66}$	50	66	115,901741	1293,56	2390,879	1,85E+00
$^{118}_{50}Sn_{68}$	50	68	117,901603	1229,666	2280,342	1,85E+00
$^{120}_{50}Sn_{70}$	50	70	119,9021947	1171,34	2194,299	1,87E+00
$^{122}_{50}Sn_{72}$	50	72	121,903439	1140,55	2142,06	1,88E+00
$^{124}_{50}Sn_{74}$	50	74	123,9052739	1131,739	2101,711	1,86E+00
$^{126}_{50}Sn_{76}$	50	76	125,907653	1141,15	2049,74	1,80E+00
$^{128}_{50}Sn_{78}$	50	78	127,910537	1168,83	2000,37	1,71E+00
$^{130}_{50}Sn_{80}$	50	80	129,913967	1221,26	1995,65	1,63E+00
$^{132}_{50}Sn$	50	82	131,917816	4041,1	4415,6	1,09E+00

$\bar{0}$ 82						
134 $_{sn}$ $\bar{0}$ 84	50	84	133,92829	725	1600	2,21E+00

50

$^{110}_{52}Te_{56}$	52	56	107,92944	625,4	1289	2,06E+00
$^{111}_{52}Te_{58}$	52	58	109,92241	657,7	1401,8	2,13E+00
$^{112}_{52}Te_{60}$	52	60	111,91701	689,01	1476,1	2,14E+00
$^{114}_{52}Te_{62}$	52	62	113,91209	708,9	1483,83	2,09E+00
$^{116}_{52}Te_{64}$	52	64	115,90846	678,92	1359,39	2,00E+00
$^{118}_{52}Te_{66}$	52	66	117,905828	605,706	1206,42	1,99E+00
$^{120}_{52}Te_{68}$	52	68	119,90402	560,438	1161,56	2,07E+00
$^{122}_{52}Te_{70}$	52	70	121,9030439	564,117	1181,248	2,09E+00
$^{124}_{52}Te_{72}$	52	72	123,9028179	602,731	1248,58	2,07E+00
$^{126}_{52}Te_{74}$	52	74	125,9033117	666,338	1361,39	2,04E+00
$^{128}_{52}Te_{76}$	52	76	127,9044631	743,3	1497,035	2,01E+00
$^{130}_{52}Te_{78}$	52	78	129,9062244	839,494	1632,997	1,95E+00
$^{132}_{52}Te_{80}$	52	80	131,908553	973,9	1671,29	1,72E+00
$^{134}_{52}Te_{82}$	52	82	133,911369	1279,04	1576,13	1,23E+00
$^{136}_{52}Te_{84}$	52	84	135,9201	605,91	1029	1,70E+00
$^{138}_{52}Te_{86}$	52	86	137,92922	443,1	750	1,69E+00
$^{111}_{54}Xe_{58}$	54	58	111,93562	466	1122,1	2,41E+00
$^{113}_{54}Xe_{60}$	54	60	113,92798	449,7	1069,1	2,38E+00
$^{116}_{54}Xe_{62}$	54	62	115,921581	393,5	917,9	2,33E+00
$^{118}_{54}Xe_{64}$	54	64	117,916179	337,32	810,2716	2,40E+00
$^{120}_{54}Xe_{66}$	54	66	119,911784	322,4	796,16	2,47E+00
$^{122}_{54}Xe_{68}$	54	68	121,908368	331,18	828,53	2,50E+00
$^{124}_{54}Xe_{70}$	54	70	123,905893	354,14	878,92	2,48E+00
$^{126}_{54}Xe_{72}$	54	72	125,904274	388,634	942	2,42E+00
$^{128}_{54}Xe_{74}$	54	74	127,9035313	442,91	1033,147	2,33E+00

54	74						
130	Xe	54	76	129,903508	536,085	1204,614	2,25E+00
54	76						
132	Xe	54	78	131,9041535	667,72	1440,323	2,16E+00
54	78						
134	Xe	54	80	133,9053945	847,041	1731,17	2,04E+00
54	80						
136	Xe	54	82	135,907219	1313,028	1694,386	1,29E+00
54	82						
138	Xe	54	84	137,91395	588,825	1072,53	1,82E+00
54	84						
140	Xe	54	86	139,92164	376,658	834,29	2,21E+00
54	86						
142	Xe	54	88	141,92971	287,1	690,7	2,41E+00
54	88						
144	Xe	54	90	143,93851	252,6	644,3	2,55E+00
54	90						
118	Ba	56	62	117,93304	194	554	2,86E+00
56	62						
120	Ba	56	64	119,92604	183	544	2,97E+00
56	64						
122	Ba	56	66	121,9199	196,1	568,6	2,90E+00
56	66						
124	Ba	56	68	123,915094	229,89	651,66	2,83E+00
56	68						
126	Ba	56	70	125,91125	256,09	711,1	2,78E+00
56	70						
128	Ba	56	72	127,908318	284,09	763,31	2,69E+00
56	72						
130	Ba	56	74	129,9063208	357,38	901,85	2,52E+00
56	74						
132	Ba	56	76	131,9050613	464,588	1127,615	2,43E+00
56	76						
134	Ba	56	78	133,9045084	604,723	1400,59	2,32E+00
56	78						
136	Ba	56	80	135,9045759	818,515	1866,548	2,28E+00
56	80						
138	Ba	56	82	137,9052472	1435,818	1898,614	1,32E+00
56	82						

$^{140}_{56}Ba_{84}$	56	84	139,910605	602,35	1130,6	1,88E+00
$^{142}_{56}Ba_{86}$	56	86	141,916453	359,597	834,81	2,32E+00
$^{144}_{56}Ba_{88}$	56	88	143,922953	199,326	530,19	2,66E+00
$^{146}_{56}Ba_{90}$	56	90	145,93022	181,05	513,5	2,84E+00
$^{148}_{56}Ba_{92}$	56	92	147,93772	141,7	423,1	2,99E+00

51

$^{120}_{58}Ce_{66}$	58	66	123,93041	142	447,8	3,15E+00
$^{126}_{58}Ce_{68}$	58	68	125,92397	169,59	519,04	3,06E+00
$^{128}_{58}Ce_{70}$	58	70	127,91891	207,3	606,77	2,93E+00
$^{130}_{58}Ce_{72}$	58	72	129,91474	253,99	710,37	2,80E+00
$^{132}_{58}Ce_{74}$	58	74	131,91146	325,54	858,82	2,64E+00
$^{134}_{58}Ce_{76}$	58	76	133,908925	409,12	1048,68	2,56E+00
$^{136}_{58}Ce_{78}$	58	78	135,907172	552,2	1314,15	2,38E+00
$^{138}_{58}Ce_{80}$	58	80	137,905991	788,744	1826,48	2,32E+00
$^{140}_{58}Ce_{82}$	58	82	139,9054387	1596,227	2083,26	1,31E+00
$^{142}_{58}Ce_{84}$	58	84	141,909244	641,286	1219,37	1,90E+00
$^{144}_{58}Ce_{86}$	58	86	143,913647	397,441	938,65	2,36E+00
$^{146}_{58}Ce_{88}$	58	88	145,91876	258,46	668,31	2,59E+00
$^{148}_{58}Ce_{90}$	58	90	147,92443	158,468	453,45	2,86E+00
$^{150}_{58}Ce_{92}$	58	92	149,93041	97,1	305,7	3,15E+00
$^{152}_{58}Ce_{94}$	58	94	151,93654	81,7	264	3,23E+00
$^{120}_{60}Nd_{68}$	60	68	127,93539	133,66	424,47	3,18E+00
$^{130}_{60}Nd_{70}$	60	70	129,92851	158	485,5	3,07E+00
$^{132}_{60}Nd_{72}$	60	72	131,923321	212,62	610,85	2,87E+00
$^{134}_{60}Nd_{74}$	60	74	133,91879	294,3	788,92	2,68E+00
$^{136}_{60}Nd_{76}$	60	76	135,914976	373,6	976,37	2,61E+00
$^{138}_{60}Nd_{78}$	60	78	137,91195	520,1	1249,87	2,40E+00
$^{140}_{60}Nd_{80}$	60	80	139,90955	773,73	1801,9	2,33E+00
$^{142}_{60}Nd_{82}$	60	82	141,9077233	1575,83	2100,787	1,33E+00
$^{144}_{60}Nd_{84}$	60	84	143,9100873	696,513	1314,669	1,89E+00

$^{146}_{60}Nd_{86}$	60	86	145,9131169	453,77	1042,22	2,30E+00
$^{148}_{60}Nd_{88}$	60	88	147,916893	301,702	752,29	2,49E+00
$^{150}_{60}Nd_{90}$	60	90	149,920891	130,21	381,1	2,93E+00
$^{152}_{60}Nd_{92}$	60	92	151,924682	72,51	236,54	3,26E+00
$^{154}_{60}Nd_{94}$	60	94	153,92948	70,8	233,2	3,29E+00
$^{156}_{60}Nd_{96}$	60	96	155,93502	66,9	222,2	3,32E+00
$^{130}_{62}Sm_{68}$	62	68	129,94892	122		
$^{132}_{62}Sm_{70}$	62	70	131,94069	131	417	3,18E+00
$^{134}_{62}Sm_{72}$	62	72	133,93397	163	479	2,94E+00
$^{136}_{62}Sm_{74}$	62	74	135,928276	254,91	686,36	2,69E+00
$^{138}_{62}Sm_{76}$	62	76	137,923244	346,9	891,6	2,57E+00
$^{140}_{62}Sm_{78}$	62	78	139,918995	530,7	1245,83	2,35E+00
$^{142}_{62}Sm_{80}$	62	80	141,915198	768	1791,4	2,33E+00
$^{144}_{62}Sm_{82}$	62	82	143,911999	1660,2	2190,891	1,32E+00
$^{146}_{62}Sm_{84}$	62	84	145,913041	747,115	1381,28	1,85E+00
$^{148}_{62}Sm_{86}$	62	86	147,9148227	550,265	1180,261	2,14E+00
$^{150}_{62}Sm_{88}$	62	88	149,9172755	333,863	773,374	2,32E+00
$^{152}_{62}Sm_{90}$	62	90	151,9197324	121,7817	366,48	3,01E+00
$^{154}_{62}Sm_{92}$	62	92	153,9222093	81,976	266,817	3,25E+00
$^{156}_{62}Sm_{94}$	62	94	155,925528	75,89	249,71	3,29E+00
$^{158}_{62}Sm_{96}$	62	96	157,92999	72,8	240,3	3,30E+00
$^{160}_{62}Sm_{98}$	62	98	159,93514	70,6	233,3	3,30E+00
$^{138}_{64}Gd_{74}$	64	74	137,94012	220,9	605,2	2,74E+00
$^{140}_{64}Gd_{76}$	64	76	139,93367	328,6	836,2	2,54E+00

Gd	*6*					
4						

52

$^{142}_{64}Gd_{78}$	64	78	141,92812	515,3	1208,8	2,35E+00
$^{144}_{64}Gd_{80}$	64	80	143,92296	743	1744,52	2,35E+00
$^{146}_{64}Gd_{82}$	64	82	145,918311	1971,97	2611,39	1,32E+00
$^{148}_{64}Gd_{84}$	64	84	147,918115	784,43	1416,38	1,81E+00
$^{150}_{64}Gd_{86}$	64	86	149,918659	638,045	1288,42	2,02E+00
$^{152}_{64}Gd_{88}$	64	88	151,919791	344,2789	755,39	2,19E+00
$^{154}_{64}Gd_{90}$	64	90	153,9208656	123,0714	370,99	3,01E+00
$^{156}_{64}Gd_{92}$	64	92	155,9221227	88,9666	288,187	3,24E+00
$^{158}_{64}Gd_{94}$	64	94	157,9241039	79,51	261,46	3,29E+00
$^{160}_{64}Gd_{96}$	64	96	159,9270541	75,26	248,52	3,30E+00
$^{162}_{64}Gd_{98}$	64	98	161,930985	71	236,4	3,33E+00
$^{142}_{66}Dy_{76}$	66	76	141,94637	315,9	798,9	2,53E+00
$^{144}_{66}Dy_{78}$	66	78	143,93925	492,5	1165	2,37E+00
$^{146}_{66}Dy_{80}$	66	80	145,932845	682,9	1608,2	2,35E+00
$^{148}_{66}Dy_{82}$	66	82	147,92715	1677,3	2426,7	1,45E+00
$^{150}_{66}Dy_{84}$	66	84	149,925585	803,4	1456,6	1,81E+00
$^{152}_{66}Dy_{86}$	66	86	151,924718	613,81	1261,2	2,05E+00
$^{154}_{66}Dy_{88}$	66	88	153,924424	334,58	746,78	2,23E+00
$^{156}_{66}Dy_{90}$	66	90	155,924283	137,83	404,19	2,93E+00
$^{158}_{66}Dy_{92}$	66	92	157,924409	98,918	317,139	3,21E+00
$^{160}_{66}Dy_{94}$	66	94	159,9251975	86,7882	283,32	3,26E+00

162 Dy 66 96	66	96	161,9267984	80,66	265,664	3,29E+00
164 Dy 66 98	66	98	163,9291748	73,392	242,231	3,30E+00
166 Dy 66 100	66	100	165,9328067	76,587	253,53	3,31E+00
144 Er 68 76	68	76	143,96038	330		
146 Er 68 78	68	78	145,952			
148 Er 68 80	68	80	147,94455	646,6	1522,68	2,35E+00
150 Er 68 82	68	82	149,937914	1578,87	2293,9	1,45E+00
152 Er 68 84	68	84	151,93505	808,27	1480,9	1,83E+00
154 Er 68 86	68	86	153,932783	560	1162,2	2,08E+00
156 Er 68 88	68	88	155,931065	344,51	797,39	2,31E+00
158 Er 68 90	68	90	157,929893	192,15	527,22	2,74E+00
160 Er 68 92	68	92	159,929083	125,8	389,9	3,10E+00
162 Er 68 94	68	94	161,928778	102,04	329,62	3,23E+00
164 Er 68 96	68	96	163,9292	91,4	299,43	3,28E+00
166 Er 68 98	68	98	165,9302931	80,577	264,99	3,29E+00
168 Er 68 100	68	100	167,9323702	79,804	264,089	3,31E+00
170 Er 68 102	68	102	169,9354643	78,591	260,148	3,31E+00
172 Er 68 104	68	104	171,939356	77	255	3,31E+00
152 Yb	70	82	151,95029	1531,4		

$\bar{0}$ 82						
$^{154}_{Yb}$ $\bar{0}$ 84	70	84	153,946394	821,3	1516	1,85E+00
$^{156}_{Yb}$ $\bar{0}$ 86	70	86	155,942818	536,4	1143,2	2,13E+00
$^{158}_{Yb}$ $\bar{0}$ 88	70	88	157,939866	358,2	835,2	2,33E+00
$^{160}_{Yb}$ $\bar{0}$ 90	70	90	159,937552	243,1	638,4	2,63E+00
$^{162}_{Yb}$ $\bar{0}$ 92	70	92	161,935768	166,85	487,33	2,92E+00
$^{164}_{Yb}$ $\bar{0}$ 94	70	94	163,934489	123,36	385,56	3,13E+00
$^{166}_{Yb}$ $\bar{0}$ 96	70	96	165,933882	102,37	330,48	3,23E+00
$^{168}_{Yb}$ $\bar{0}$ 98	70	98	167,933897	87,73	286,551	3,27E+00

53

17 $0_{70}^{Yb}100$	70	100	169,9347618	84,25474	277,43	3,29E+00
17 $2_{70}^{Yb}102$	70	102	171,9363815	78,7427	260,268	3,31E+00
174 $_{70}^{Yb}104$	70	104	173,9388621	76,471	253,117	3,31E+00
176 $_{70}^{Yb}106$	70	106	175,9425717	82,13	271,85	3,31E+00
178 $_{70}^{Yb}108$	70	108	177,946647	84	278	3,31E+00
15 $4_{72}^{Hf}82$	72	82	153,96486	1513		
15 $6_{72}Hf_{84}$	72	84	155,95936	858	1585,2	1,85E+00
15 $8_{72}^{Hf}86$	72	86	157,954799	476,36	1033,33	2,17E+00
16 $0_{72}Hf_{88}$	72	88	159,950684	389,6	898,26	2,31E+00
16 $2_{72}^{Hf}90$	72	90	161,94721	285	729,5	2,56E+00
16 $4_{72}Hf_{92}$	72	92	163,944367	211,05	587,1	2,78E+00
16 $6_{72}^{Hf}94$	72	94	165,94218	158,5	470,46	2,97E+00
16 $8_{72}Hf_{96}$	72	96	167,94057	124	385,92	3,11E+00
17 $0_{72}Hf_{98}$	72	98	169,93961	100,8	321,99	3,19E+00
17 $^{2}_{72}Hf_{100}$	72	100	171,939448	95,22	309,24	3,25E+00
17 $^{4}_{72}Hf_{102}$	72	102	173,940046	90,985	297,38	3,27E+00
17 $^{6}_{72}Hf_{104}$	72	104	175,9414086	88,351	290,18	3,28E+00
17 $^{8}_{72}Hf_{106}$	72	106	177,9436988	93,18	306,6182	3,29E+00
18 $^{0}_{72}Hf_{108}$	72	108	179,94655	93,326	308,579	3,31E+00
18 $^{2}_{72}Hf_{110}$	72	110	181,950554	97,79	322,17	3,29E+00
18 $^{4}_{72}Hf_{112}$	72	112	183,95545	107,4	349,6	3,26E+00
162 $_{74}^{W}88$	74	88	161,963497	450,2		
164 $_{74}^{W}90$	74	90	163,958954	331,6	823,7	2,48E+00

$^{166}_{74}W_{92}$	74	92	165,955027	251,7	675,7	2,68E+00
$^{168}_{74}W_{94}$	74	94	167,951808	199,3	562,3	2,82E+00
$^{170}_{74}W_{96}$	74	96	169,949228	156,85	462,33	2,95E+00
$^{172}_{74}W_{98}$	74	98	171,94729	123,2	377,1	3,06E+00
$^{174}_{74}W_{100}$	74	100	173,94608	113	356,4	3,15E+00
$^{176}_{74}W_{102}$	74	102	175,94563	109,08	348,2	3,19E+00
$^{178}_{74}W_{104}$	74	104	177,945876	106,06	342,74	3,23E+00
$^{180}_{74}W_{106}$	74	106	179,946704	103,557	337,516	3,26E+00
$^{182}_{74}W_{108}$	74	108	181,9482042	100,106	329,4268	3,29E+00
$^{184}_{74}W_{110}$	74	110	183,9509312	111,208	364,069	3,27E+00
$^{186}_{74}W_{112}$	74	112	185,9543641	122,33	396,547	3,24E+00
$^{188}_{74}W_{114}$	74	114	187,958489	143	439,49	3,07E+00
$^{190}_{74}W_{116}$	74	116	189,96318	205	564	2,75E+00
$^{164}_{76}Os_{88}$	76	88	163,97804	548	1206,3	2,20E+00
$^{166}_{76}Os_{90}$	76	90	165,972691	430,8	1021	2,37E+00
$^{168}_{76}Os_{92}$	76	92	167,967804	341,2	857,3	2,51E+00
$^{170}_{76}Os_{94}$	76	94	169,963577	286,7	749,9	2,62E+00
$^{172}_{76}Os_{96}$	76	96	171,960023	277,77	606,17	2,18E+00
$^{174}_{76}Os_{98}$	76	98	173,957062	158,7	435	2,74E+00
$^{176}_{76}Os_{100}$	76	100	175,95481	135,1	395,5	2,93E+00
$^{178}_{76}Os_{102}$	76	102	177,953251	131,6	398,79	3,03E+00
$^{180}_{76}Os_{104}$	76	104	179,952379	132,3	408,62	3,09E+00
$^{182}_{76}Os_{106}$	76	106	181,95211	127	400,29	3,15E+00
$^{184}_{76}Os_{108}$	76	108	183,9524891	119,8	383,68	3,20E+00
$^{186}_{76}Os_{110}$	76	110	185,9538382	137,159	434,087	3,16E+00

188 $_{76}Os_{112}$	76	112	187,9558382	155,021	477,94	3,08E+00
190 $_{76}Os_{114}$	76	114	189,958447	186,718	547,854	2,93E+00
192 $_{76}Os_{116}$	76	116	191,9614807	205,79561	580,28	2,82E+00
194 $_{76}Os_{118}$	76	118	193,9651821	218,509	601	2,75E+00
196 $_{76}Os_{120}$	76	120	195,96964	300	760	2,53E+00
168 $_{78}Pt_{90}$	78	90	167,98815	582	1307,3	2,25E+00
170 $_{78}Pt_{92}$	78	92	169,982495	509	1171,2	2,30E+00
172 $_{78}Pt_{94}$	78	94	171,977347	457	1069,98	2,34E+00
174 $_{78}Pt_{96}$	78	96	173,972819	394	891,8	2,26E+00
176 $_{78}Pt_{98}$	78	98	175,968945	263,9	564,1	2,14E+00
178 $_{78}Pt_{100}$	78	100	177,965649	170,1	427,4	2,51E+00
180 $_{78}Pt_{102}$	78	102	179,963031	152,23	410,74	2,70E+00
182 $_{78}Pt_{104}$	78	104	181,961171	154,9	419,62	2,71E+00
184 $_{78}Pt_{106}$	78	106	183,959922	162,97	435,91	2,67E+00
186 $_{78}Pt_{108}$	78	108	185,959351	191,53	490,33	2,56E+00
188 $_{78}Pt_{110}$	78	110	187,959395	265,63	671,01	2,53E+00
190 $_{78}Pt_{112}$	78	112	189,959932	295,8	737,04	2,49E+00
192 $_{78}Pt_{114}$	78	114	191,961038	316,50819	784,5759	2,48E+00
194 $_{78}Pt_{116}$	78	116	193,9626803	328,453	811,269	2,47E+00
196 $_{78}Pt_{118}$	78	118	195,9649515	355,6841	876,865	2,47E+00
198 $_{78}Pt_{120}$	78	120	197,967893	407,22	985,07	2,42E+00

200 Pt 78 122	78	122	199,971441	470,1	1103,3	2,35E+00
176 $_{80}Hg_{96}$	80	96	175,987355	613,3	1369,7	2,23E+00
178 $_{80}Hg_{98}$	80	98	177,982483	558,3	1012,4	1,81E+00
180 Hg 80 100	80	100	179,978266	434,1	706,7	1,63E+00
182 Hg 80 102	80	102	181,97469	351,8	613,2	1,74E+00
184 Hg 80 104	80	104	183,971713	366,51	653,77	1,78E+00
186 Hg 80 106	80	106	185,969362	405,33	807,99	1,99E+00
188 Hg 80 108	80	108	187,967577	412,8	1004,8	2,43E+00
190 Hg 80 110	80	110	189,966322	416,4	1041,77	2,50E+00
192 Hg 80 112	80	112	191,965634	422,8	1057,58	2,50E+00
194 Hg 80 114	80	114	193,965439	428	1064,19	2,49E+00
196 Hg 80 116	80	116	195,965833	425,98	1061,44	2,49E+00
198 Hg 80 118	80	118	197,966769	411,80249	1048,49	2,55E+00
200 Hg 80 120	80	120	199,968326	367,944	947,24	2,57E+00
202 Hg 80 122	80	122	201,970643	439,562	1119,84	2,55E+00
204 Hg 80 124	80	124	203,9734939	436,552	1128,23	2,58E+00
206 Hg 80 126	80	126	205,977514	1068,54		
182 Pb 82 100	82	100	181,992672	888,3	1119,5	1,26E+00
184 Pb 82 102	82	102	183,988142	701,5	938,9	1,34E+00
186 Pb 82 104	82	104	185,984239	662,4	923	1,39E+00
188 Pb	82	106	187,980874	723,9	1064,7	1,47E+00

$^{190}_{82}Pb_{108}$	82	108	189,978082	773,8	1229,1	1,59E+00
$^{192}_{82}Pb_{110}$	82	110	191,975785	853,6	1355,5	1,59E+00
$^{194}_{82}Pb_{112}$	82	112	193,974012	965,35	1540,03	1,60E+00
$^{196}_{82}Pb_{114}$	82	114	195,972774	1049,2	1738,27	1,66E+00
$^{198}_{82}Pb_{116}$	82	116	197,972034	1063,5	1625,9	1,53E+00
$^{200}_{82}Pb_{118}$	82	118	199,971827	1026,62	1488,95	1,45E+00

55

$^{202}_{82}Pb_{120}$	82	120	201,972159	960,66	1382,84	1,44E+00
$^{204}_{82}Pb_{122}$	82	122	203,9730436	899,171	1274,13	1,42E+00
206 Pb 82 124	82	124	205,9744653	803,1	1683,99	2,10E+00
208 Pb 82 126	82	126	207,9766521	4085,4	4323,926	1,06E+00
210 Pb 82 128	82	128	209,9841885	799,7	1097,7	1,37E+00
212 Pb 82 130	82	130	211,9918975	804,9	1117	1,39E+00
214 Pb 82 132	82	132	213,9998054	836	1179	1,41E+00
192 Po 84 108	84	108	191,991335	262	605,2	2,31E+00
194 Po 84 110	84	110	193,988186	318,6	686,5	2,15E+00
196 Po 84 112	84	112	195,985535	463,12	890,99	1,92E+00
198 Po 84 114	84	114	197,983389	605	1158,39	1,91E+00
200 Po 84 116	84	116	199,981799	665,9	1276,9	1,92E+00
202 Po 84 118	84	118	201,980758	677,3	1248,6	1,84E+00
204 Po 84 120	84	120	203,980318	684,342	1200,661	1,75E+00
206 Po 84 122	84	122	205,980481	700,66	1177,8	1,68E+00
208 Po 84 124	84	124	207,9812457	686,528	1346,56	1,96E+00
210 Po 84 126	84	126	209,9828737	1181,4	1426,701	1,21E+00
212 Po 84 128	84	128	211,988868	727,33	1132,53	1,56E+00
214 Po 84 130	84	130	213,9952014	609,316	1015,039	1,67E+00
216 Po 84 132	84	132	216,001915	549,76	968,94	1,76E+00
218 Po 84 134	84	134	218,008973	511	935,2	1,83E+00
198 Rn 86 112	86	112	197,998679	339	749,5	2,21E+00
200 Rn 86 114	86	114	199,995699	432,9	936,3	2,16E+00

6						
202 Rn 86 116	86	116	201,993263	504,1	1073,1	2,13E+00
204 Rn 86 118	86	118	203,991429	542,9	1131,5	2,08E+00
206 Rn 86 120	86	120	205,990214	575,3	1134,3	1,97E+00
208 Rn 86 122	86	122	207,989642	635,8	1188,9	1,87E+00
210 Rn 86 124	86	124	209,989696	643,8	1461,6	2,27E+00
212 Rn 86 126	86	126	211,990704	1273,8	1501,6	1,18E+00
214 Rn 86 128	86	128	213,995363	694,7	1141,2	1,64E+00
216 Rn 86 130	86	130	216,000274	461,9	840,5	1,82E+00
218 Rn 86 132	86	132	218,0056013	324,22	653,18	2,01E+00
220 Rn 86 134	86	134	220,011394	240,986	533,68	2,21E+00
222 Rn 86 136	86	136	222,0175777	186,211	448,37	2,41E+00
206 Ra 88 118	88	118	206,003827	474,3	1052,1	2,22E+00
208 Ra 88 120	88	120	208,00184	520,2	1093,6	2,10E+00
210 Ra 88 122	88	122	210,000495	603,3	1205,1	2,00E+00
212 Ra 88 124	88	124	211,999794	629,3	1454,3	2,31E+00
214 Ra 88 126	88	126	214,000108	1382,4	1639,6	1,19E+00
216 Ra 88 128	88	128	216,003533	688,2	1164,1	1,69E+00
218 Ra 88 130	88	130	218,00714	389,1	741,1	1,90E+00
220 Ra 88 132	88	132	220,011028	178,47	410,07	2,30E+00

$^{222}_{88}Ra_{134}$	88	134	222,015375	111,12	301,39	2,71E+00
$^{224}_{88}Ra_{136}$	88	136	224,0202118	84,373	250,783	2,97E+00
$^{226}_{88}Ra_{138}$	88	138	226,0254098	67,67	211,54	3,13E+00
$^{228}_{88}Ra_{140}$	88	140	228,0310703	63,823	204,702	3,21E+00
$^{230}_{88}Ra_{142}$	88	142	230,037056	57,4	188,64	3,29E+00

56

$^{216}_{90}Th_{126}$	90	126	216,011062	1478	1813,8	1,23E+00
$^{218}_{90}Th_{128}$	90	128	218,013284	689,6	1194,2	1,73E+00
$^{220}_{90}Th_{130}$	90	130	220,015748	373,3	759,8	2,04E+00
$^{222}_{90}Th_{132}$	90	132	222,018468	183,3	439,8	2,40E+00
$^{224}_{90}Th_{134}$	90	134	224,021467	98,1	284,1	2,90E+00
$^{226}_{90}Th_{136}$	90	136	226,024903	72,2	226,43	3,14E+00
$^{228}_{90}Th_{138}$	90	138	228,0287411	57,759	186,838	3,23E+00
$^{230}_{90}Th_{140}$	90	140	230,0331338	53,2	174,111	3,27E+00
$^{232}_{90}Th_{142}$	90	142	232,0380553	49,369	162,12	3,28E+00
$^{234}_{90}Th_{144}$	90	144	234,043601	49,55	163,05	3,29E+00
$^{226}_{92}U_{134}$	92	134	226,029339	80,5	250	3,11E+00
$^{228}_{92}U_{136}$	92	136	228,031374	59		
$^{230}_{92}U_{138}$	92	138	230,03394	51,72	169,34	3,27E+00
$^{232}_{92}U_{140}$	92	140	232,0371562	47,572	156,656	3,29E+00
$^{234}_{92}U_{142}$	92	142	234,0409521	43,498	143,352	3,30E+00
$^{236}_{92}U_{144}$	92	144	236,045568	45,242	149,477	3,30E+00
$^{238}_{92}U_{146}$	92	146	238,0507882	44,91	148,38	3,30E+00
$^{240}_{92}U_{148}$	92	148	240,056592	45	150,6	3,35E+00
$^{236}_{94}Pu_{142}$	94	142	236,046058	44,63	147,45	3,30E+00
$^{238}_{94}Pu_{144}$	94	144	238,0495599	44,08	145,952	3,31E+00
$^{240}_{94}Pu_{146}$	94	146	240,0538135	42,824	141,69	3,31E+00
$^{242}_{94}Pu_{148}$	94	148	242,0587426	44,54	147,3	3,31E+00
$^{244}_{94}Pu_{150}$	94	150	244,064204	46	155	3,37E+00
$^{246}_{94}Pu_{152}$	94	152	246,070205	44,2	154,5	3,50E+00
$^{238}_{96}Cm_{142}$	96	142	238,05303	35		
$^{240}_{96}Cm_{144}$	96	144	240,0555295	38		
$^{242}_{96}Cm$	96	146	242,0588358	42,13	137	3,25E+00

96 146						
$^{244}_{96}Cm_{148}$	96	148	244,0627526	42,965	142,348	3,31E+00
$^{246}_{96}Cm_{150}$	96	150	246,0672237	42,852	141,989	3,31E+00
$^{248}_{96}Cm_{152}$	96	152	248,072349	43,38	143,8	3,31E+00
$^{250}_{96}Cm_{154}$	96	154	250,078357	43		
$^{244}_{98}Cf_{146}$	98	146	244,066001	40		
$^{246}_{98}Cf_{148}$	98	148	246,0688053	44		
$^{248}_{98}Cf_{150}$	98	150	248,072185	41,53	137,81	3,32E+00
$^{250}_{98}Cf_{152}$	98	152	250,0764061	42,722	141,875	3,32E+00
$^{252}_{98}Cf_{154}$	98	154	252,081626	45,72	151,74	3,32E+00
$^{248}_{100}Fm_{148}$	100	148	248,077186	46	152	3,30E+00
$^{250}_{100}Fm_{150}$	100	150	250,079521	44		
$^{252}_{100}Fm_{152}$	100	152	252,082467	46,6		
$^{254}_{100}Fm_{154}$	100	154	254,0868544	44,988	149,35	3,32E+00
$^{256}_{100}Fm_{156}$	100	156	256,091774	48,3	159,9	3,31E+00

[i] The 'yrast' state refers to the lowest excitation state for a given angular momentum or spin in a nucleus.